Research

New Phytologist

A fungal plant pathogen overcomes *mlo*-mediated broad-spectrum disease resistance by rapid gene loss

Stefan Kusch, Lamprinos Frantzeskakis, Birthe D. Lassen, Florian Kümmel, Lina Pesch, Mirna Barsoum, Kim D. Walden and Ralph Panstruga

Unit of Plant Molecular Cell Biology, Institute for Biology I, RWTH Aachen University, Worringerweg 1, D-52056, Aachen, Germany

Author for correspondence:
Ralph Panstruga
Email: panstruga@bio1.rwth-aachen.de

Received: *14 May 2024*
Accepted: *3 August 2024*

New Phytologist (2024) **244:** 962–979
doi: 10.1111/nph.20063

Key words: adaptation, experimental evolution, genome, plant immunity, powdery mildew, rapid evolution.

Summary

- Hosts and pathogens typically engage in a coevolutionary arms race. This also applies to phytopathogenic powdery mildew fungi, which can rapidly overcome plant resistance and perform host jumps.
- Using experimental evolution, we show that the powdery mildew pathogen *Blumeria hordei* is capable of breaking the agriculturally important broad-spectrum resistance conditioned by barley loss-of-function *mlo* mutants.
- Partial *mlo* virulence of evolved *B. hordei* isolates is correlated with a distinctive pattern of adaptive mutations, including small-sized (*c.* 8–40 kb) deletions, of which one is linked to the *de novo* insertion of a transposable element. Occurrence of the mutations is associated with a transcriptional induction of effector protein-encoding genes that is absent in *mlo*-avirulent isolates on *mlo* mutant plants. The detected mutational spectrum comprises the same loci in at least two independently isolated *mlo*-virulent isolates, indicating convergent multigenic evolution. The mutational events emerged in part early (within the first five asexual generations) during experimental evolution, likely generating a founder population in which incipient *mlo* virulence was later stabilized by additional events.
- This work highlights the rapid dynamic genome evolution of an obligate biotrophic plant pathogen with a transposon-enriched genome.

Introduction

Pathogens and their hosts are locked in a coevolutionary competition where the host attempts to prevent pathogen infection, while the pathogen adapts to evade host recognition and retain its ability to infect the host. Generalist pathogens are capable to colonize a broad range of hosts, and their genomes evolve in response to selection by many hosts under diffuse coevolution (Ebert & Fields, 2020). Specialist pathogens, on the other hand, infect one or few hosts and are engaged in an intimate coevolutionary arms race. The gene-for-gene hypothesis is a paradigm for the arms race between plants and their pathogens (Flor, 1971). Plants have intracellular nucleotide-binding oligomerization domain (NOD)-like receptors (NLRs) that can recognize pathogen effectors and mount an effective defense response, while pathogens evolve to subvert or circumvent perception (Jones & Dangl, 2006). Obligate biotrophic pathogens depend on living host cells and, thus, have to evade recognition by NLRs for their very survival and reproduction. Such specialist pathogens often rapidly overcome resistance conferred by effector recognition via cognate host NLRs. For example, the obligate biotrophic barley powdery mildew fungus *Blumeria hordei* frequently escapes resistance conditioned by alleles of *Mildew locus a* (*Mla*)-encoded NLRs in barley (*Hordeum vulgare*) (Brown, 2015). Mla immune receptors directly bind secreted *B. hordei* effector proteins, and loss of recognition happens by loss or modification of the cognate effector due to spontaneous mutations in the fungal genome (Lu *et al.*, 2016; Saur *et al.*, 2019). In addition, copy number variation of effector genes contributes to genetic variation and can lead to outbreaks of new strains of filamentous plant pathogens (Qutob *et al.*, 2009; Hartmann & Croll, 2017).

Short generation times, large effective population sizes, and plastic genome architectures are drivers of rapid adaptation in microbial pathogens (Frantzeskakis *et al.*, 2020). Within the lifetime of a plant, pathogens can go through tens or even hundreds of generation cycles and can produce thousands to millions of individual mito- and meiospores as offspring (Tellier *et al.*, 2014). Hence, the standing genetic variation of the pathogen population is much larger than that of its host by default. This is likely a prerequisite for pathogen survival, since recognition of a single effector suffices to prevent proliferation and reproduction.

The genomes of filamentous plant pathogens frequently exhibit special architectures and features including dispensable accessory chromosomes and hypervariable mini-chromosomes (Langner *et al.*, 2021). These are often enriched with transposable elements, carry effector genes, and are otherwise gene-poor. Binary genome compartmentalization, known as two-speed

architecture, is characterized by distinct transposable element-rich regions that mainly contain effector genes that evolve at a faster pace than the rest of the genome (Raffaele *et al.*, 2010; Dong *et al.*, 2015). Intriguingly, some fungal plant pathogens including the cereal powdery mildew pathogen *Blumeria* harbor genomes that are massively inflated by transposable elements (Frantzeskakis *et al.*, 2018; Müller *et al.*, 2019, 2021). Transposable elements are equally distributed throughout these genomes, which are further characterized by extensive copy number variation of effector genes and the loss of some conserved ascomycete genes (Spanu *et al.*, 2010; Frantzeskakis *et al.*, 2018). In particular, long interspersed nuclear element (LINE) and long terminal repeat (LTR) retrotransposons are highly abundant, and these elements exhibit mostly very low sequence divergence, suggesting that recent transposon bursts shaped the genome of *B. hordei* (Frantzeskakis *et al.*, 2018).

At least 900 species of powdery mildew fungi (Ascomycota, *Erysiphaceae*) infect > 10 000 plant species world-wide (Braun & Cook, 2012; Kusch *et al.*, 2024), including crops, trees, and herbs (Glawe, 2008). These pathogens cause significant yield losses if not held in check by fungicides, affecting grain yield and quality (Dean *et al.*, 2012). Even though powdery mildews apparently occur as homogenous strains due to their dominating asexual mode of propagation, they can have a complex population structure with many different haplotypes present within a supposedly clonal isolate (Barsoum *et al.*, 2020).

The loss-of-function mutation of *Mildew locus o* (*Mlo*) gene(s) confers highly effective and durable broad-spectrum resistance against powdery mildew in many plant species (Kusch & Panstruga, 2017). Pathogenesis is terminated before fungal host cell entry on *mlo* mutants, which have been used widely in European barley agriculture since the late 1970s (Jørgensen, 1992). *Mlo* genes encode seven-transmembrane domain proteins (Büschges *et al.*, 1997; Devoto *et al.*, 2003) with a cytosolic calmodulin-binding domain in the carboxy-terminus (Kim *et al.*, 2002) and function as cation channels (Gao *et al.*, 2022). Genetic suppressors of *mlo*-based resistance cause partial susceptibility to powdery mildew. These include mutants of the *Required for mlo-specified resistance* (*Ror*) genes in barley (Freialdenhoven *et al.*, 1996; Collins *et al.*, 2003; Acevedo-Garcia *et al.*, 2022) as well as *PENETRATION* (*PEN*) genes in *Arabidopsis thaliana*, which are major components of prepenetration resistance to powdery mildew (Collins *et al.*, 2003; Lipka *et al.*, 2005; Stein *et al.*, 2006; Hématy *et al.*, 2020). In addition, abiotic stress conditions can result in a temporary breakdown of *mlo*-based resistance (Newton & Young, 1996; Schwarzbach, 2001). The Japanese *B. hordei* isolate RACE1 is the only known natural case with partial virulence on barley *mlo* mutant plants (Jørgensen & Wolfe, 1994; Lyngkjær *et al.*, 1995). In addition, a previous experimental evolution approach revealed several partially *mlo*-virulent *B. hordei* isolates (Schwarzbach, 1979). Molecular analysis of these *B. hordei* isolates indicated that the *mlo* virulence phenotype depends on a small number of unidentified genes (Atzema, 1998; Grell *et al.*, 2005), but the underlying mechanism remains elusive.

To close this gap in knowledge, we here deployed real-time evolution experiments to select a set of *mlo*-virulent *B. hordei* isolates for detailed molecular analysis. We identified a distinctive pattern of few convergent mutational events in the three identified isolates, resulting in an altered transcriptional program during fungal pathogenesis on barley *mlo* mutant plants. Our data suggest that the majority of mutational events occurred early in our experimental setup and rapidly outcompeted the respective parental alleles. Enhanced *B. hordei* virulence on *mlo* mutants seems to be correlated with a fitness cost in the form of lowered virulence on barley wild-type (WT) plants, which may explain why the *mlo*-virulent phenotype does not prevail under agricultural conditions. Collectively, our findings provide an example of how few mutations in the genome of a phytopathogen can cause a drastic change in its virulence spectrum, enabling its rapid adaptation to new host environments.

Materials and Methods

Plant growth conditions

All plants were cultivated in SoMi513 soil (HAWITA, Vechta, Germany). Healthy barley (*Hordeum vulgare* L.) and wheat (*Triticum aestivum* L.) plants were grown under a long day cycle (16 h : 8 h, 23°C : 20°C, light : dark) with 60–65% relative humidity (RH) at a light intensity of 105–120 µmol s^{-1} m^{-2}. *Arabidopsis thaliana* (L.) Heynh. plants were cultivated under a short-day cycle (8 h : 16 h, 22°C : 20°C, light : dark), at 80–90% RH, and a light intensity of 100 µmol s^{-1} m^{-2}. For powdery mildew infection assays, the plants were transferred to isolate-specific infection chambers with a long day cycle (12 h : 12 h, 20°C : 19°C, light : dark), *c.* 60% relative humidity and 100 µmol s^{-1} m^{-2}.

Experimental evolution approach

We obtained *mlo*-virulent *Blumeria hordei* M. Liu & Hambl., 2021 in (Liu *et al.*, 2021) isolates derived from the *mlo*-avirulent parental strain *B. hordei* $K1_{AC}$ (Barsoum *et al.*, 2020) following a previously described approach (Schwarzbach, 1979). Briefly, we selected for *mlo* virulence by heavily inoculating barley *mlo* plants and, after 1–2 wk, recovered the occasionally occurring colonies by subsequent inoculation of the susceptible (*Mlo* genotype) cultivar (cv) Ingrid to proliferate fungal biomass. After 1 wk, we again re-inoculated on *mlo* plants. We repeated the procedure up until the 15^{th} inoculation on *mlo* plants (Generation 15), after which the obtained *B. hordei* isolates were cultivated on barley *mlo* mutant plants exclusively. Conidia were collected toward whole-genome DNA sequencing after 5, 10, and 50 generations on *mlo* plants.

Powdery mildew infection assays

One-week-old barley and wheat plants and 4–5-wk-old *A. thaliana* plants (rosette size of 2–2.5 cm) were used for powdery mildew infection assays with *B. hordei* (isolates A6 (Wiberg, 1974),

DH14 (Spanu *et al.*, 2010), $K1_{AC}$ (Barsoum *et al.*, 2020), $K1_{CGN}$ (Hinze *et al.*, 1991), and RACE1 (Lyngkjær *et al.*, 1995)) or the wheat pathogen *Blumeria graminis* (DC.) Speer f. sp. *tritici* (E.J. Marchal) (isolate Bgt_{AC} (Acevedo-Garcia *et al.*, 2017)). The powdery mildew conidiospores were blown onto the plants in an infection tower; spores were allowed to settle for 10–15 min. Inoculated plants were incubated in the respective *B. hordei* infection chamber. The samples for host cell penetration assays were bleached in 80% ethanol at 48 h post inoculation (hpi). The leaves were submerged twice in Coomassie staining solution (45% v/v MeOH, 10% v/v acetic acid, 0.05% w/v Coomassie blue R-250; Carl Roth, Karlsruhe, Germany) for 15–20 s, and then mounted on a glass slide with 50% glycerol. The samples were evaluated by bright-field microscopy. Leaves from four to five plants/genotype were scored for fungal penetration success with 100–200 interaction sites per leaf. Penetration success is expressed as the percentage of spores forming secondary hyphae upon interaction over spores forming an appressorium only.

For the *B. hordei*–Arabidopsis interaction assays, the leaves were stored in Aniline blue staining solution (150 mM K_2HPO_4, 0.01% w/v Aniline blue; Sigma-Aldrich, Munich, Germany) in the dark overnight to stain callose before Coomassie staining. These samples were analyzed by fluorescence microscopy with illumination by an ultraviolet (UV) lamp (bandpass 327–427 nm) and an emission filter for Aniline blue/DAPI at 417–477 nm.

Analysis of conidia shape

Conidia were collected from the surface of susceptible barley leaves at 7 d post inoculation (dpi) using transparent Scotch™ tape, which was then mounted onto a glass slide with 20 µl of tap water. Bright-field photographs were taken with the Keyence Biorevo BZ-9000 and BZII Viewer software (Keyence, Osaka, Japan) using the ×10 magnification objective. Conidia shape (length and width, area, and perimeter) was determined using the ImageJ (https://imagej.nih.gov) function Analyze Particles.

Conidia germination assay

Conidia from 7- to 10-d-old powdery mildew colonies were blown onto 1% agar-agar Kobe I (Carl Roth, Karlsruhe, Germany). Conidia germination was assessed via bright-field microscopy at 6 hpi, scoring the percentage of spores that formed primary germ tubes and counting the number of germ tubes on germinated conidia.

Whole transcriptome shotgun sequencing analysis

Epiphytic fungal material was collected as described previously (Li *et al.*, 2019) at 6 hpi (appressorium formation) and 18 hpi (early host cell penetration). Whole transcriptome shotgun sequencing (RNA-sequencing) was done by the service provider CeGaT (CeGaT, Tübingen, Germany), yielding 100-bp paired-end reads (raw data available at https://www.ncbi.nlm.nih.gov/sra under BioProject ID PRJNA639160). Raw reads were trimmed using Trimmomatic v.0.39 (Bolger *et al.*, 2014), and quality control of the reads was done with FastQC v.0.12.1 (Babraham Bioinformatics, Cambridge, UK). Hisat2 (Kim *et al.*, 2015) with '--max-intronlen 1000 -k 1' mapped the reads to the *B. hordei* DH14 reference genome (Frantzeskakis *et al.*, 2018) and the *H. vulgare* cv Morex reference genome version Morex3 (Mascher *et al.*, 2021). The SAM/BAM files were parsed with SAMtools v.1.18 (Li *et al.*, 2009) and BEDtools v.2.31.0 (Quinlan & Hall, 2010); read counts were determined using featureCounts v.2.0.1 (Liao *et al.*, 2014) with the gene annotations for *B. hordei* DH14 v.4.3 (Qian *et al.*, 2023) and Morex3 (Mascher *et al.*, 2021), respectively. Nonexpressed genes were removed with a cutoff of TPM < 1 in any sample. Differential expression analysis was performed via the limma-VOOM pipeline with cutoffs log-fold-change > |1| and $P_{adj} < 0.05$ using limma v.3.56.2 (Law *et al.*, 2016), DESeq2 v.1.40.2 (Love *et al.*, 2014), and EdgeR v.3.56.2 (Robinson *et al.*, 2010). Genes differentially expressed in *B. hordei* SK1 were compared with their expression pattern in the avirulent isolate *B. hordei* $K1_{AC}$ throughout the infection life cycle using RNA-seq time-course expression data obtained previously (Qian *et al.*, 2023). Differential expression of selected genes was verified by quantitative reverse transcription polymerase chain reaction, performed as previously described (Pennington *et al.*, 2015); primers are listed in Supporting Information Table S1.

Quantitative reverse transcriptase-polymerase chain reaction (qRT-PCR)

Detached barley leaves were placed on 1% agar-agar Kobe I (Carl Roth, Karlsruhe, Germany) plates containing 85 µM benzimidazole, and inoculated with *B. hordei* isolates $K1_{AC}$, SK1, SK2, and SK3, respectively. Epidermal peelings were collected at 0, 6, and 18 hpi in three biological replicates and flash-frozen in liquid nitrogen. RNA extraction was performed using the TRIzol protocol (Invitrogen-Thermo Fisher, Waltham, MA, USA). RNA concentration was determined using Nanodrop 2000c (Thermo Fisher Scientific, Langerwehe, Germany), and RNA integrity was assessed on a 2% agarose gel. Genomic DNA removal was done via DNase I (RNase-free; Thermo Fisher Scientific). Complementary DNA (cDNA) was synthesized using the High-Capacity RNA-to-cDNA Kit (Applied Biosystems-Thermo Fisher, Schwerte, Germany) and stored at −20°C until further use. Quantitative reverse transcription polymerase chain reaction was performed using the Takyon No ROX SYBR MasterMix blue dTTP Kit (Eurogentec, Seraing, Belgium) and the LightCycler 480 II (Roche, Rotkreuz, Switzerland). 1 : 10-diluted cDNA was used as a template for quantitative reverse transcription polymerase chain reactions. The PCR efficiency of all primers used in this study (Table S1) was between 1.8 and 2.0, and the annealing temperature was set to 58°C. Evaluation of expression levels of target genes in relation to the housekeeping gene *B. hordei GAPDH* (Pennington *et al.*, 2015) was performed using the ΔC_t method (Livak & Schmittgen, 2001), calculated as $2^{-(Ct(target)-Ct(GAPDH))}$. Each biological replicate was measured in technical triplicates.

Genome sequencing and analysis

High-molecular-weight genomic DNA from barley powdery mildew conidia was generated according to Feehan *et al.* (2017) with the modifications indicated in Frantzeskakis *et al.* (2018). DNA shotgun sequencing was performed using Illumina NovaSeq technology with 1 μg input DNA at the service provider CeGaT (CeGaT, Tübingen, Germany), yielding 150-bp paired-end reads (raw data available at https://www.ncbi.nlm.nih.gov/sra under BioProject ID PRJNA639160). Long-read sequencing by MinION (Oxford Nanopore Technologies, Oxford, USA) technology and genome assembly of *B. hordei* SK1 were done as in Frantzeskakis *et al.* (2018). Short-read sequencing data from this work and from *B. hordei* isolates sequenced previously, that is $K1_{CGN}$ and A6 (Hacquard *et al.*, 2013), and DH14 and long-read sequencing data from *B. hordei* RACE1 (Frantzeskakis *et al.*, 2018), were remapped to the *B. hordei* DH14 reference genome (Frantzeskakis *et al.*, 2018) using the function bwa mem of BWA v.0.7.17-r1188 (Li & Durbin, 2009).

Single Nucleotide Variant (SNVs), insertions, and deletions (indels) were detected with FreeBayes v.1.3.7-dirty (Garrison & Marth, 2012) and raw SNVs and indels were filtered using VCFtools v.0.1.16 (Danecek *et al.*, 2011) and BCFtools v.1.17 (https://samtools.github.io/bcftools/bcftools.html) according to Barsoum *et al.* (2020). We used SnpEff v.4.3t (build 2017-11-24 10:18) (Cingolani *et al.*, 2012) to identify SNVs and indels in genic loci with predicted effects, and manually inspected candidate polymorphisms with Integrative Genomics Viewer (IGV) browser v.2.16.1 (Robinson *et al.*, 2017). Genome mapping coverage was determined with BEDtools v.2.31.0 (Quinlan & Hall, 2010). Synteny analysis was performed using the function nucmer from MUMmer v.3.23 (Kurtz *et al.*, 2004) and visualized using the R package genoPlotR v.0.8.11 (Guy *et al.*, 2010). Gene losses and gene alleles were verified by polymerase chain reaction (PCR) on genomic DNA; primers are listed in Table S1.

Phylogenetic and functional analysis

Orthologues of *Aspergillus fumigatus* and *B. hordei medA* were identified using BlastP (https://blast.ncbi.nlm.nih.gov/Blast.cgi) at *E* value < 1E-25. Protein alignments were done with ClustalW in MegaX (Kumar *et al.*, 2016) and visualized using Jalview v.2.11.3.2 (Waterhouse *et al.*, 2009). The phylogenetic tree building was facilitated by Phylogeny Analysis at http://www.phylogeny.fr, with 100 bootstrap replications and otherwise default parameters. Functional predictions were done with InterProScan (https://www.ebi.ac.uk/interpro), NCBI CDART (https://www.ncbi.nlm.nih.gov/Structure/lexington/lexington.cgi), PROSITE (https://www.expasy.org/resources/prosite), and protein disorder by IUPRED3 (Erdős *et al.*, 2021). Protein structures were visualized with YASARA (http://www.yasara.org); structural comparison of BLGH_06723 was performed against E3 ubiquitin-protein ligase parkin of *Rattus norvegicus* (10.2210/pdb4K95/pdb/; Trempe *et al.*, 2013).

Statistical analysis

The statistics program R v.4.3.1 (R Core Team, 2018) (www.r-project.org/) was used for data analysis, statistics, and plotting. Data analysis was supported by the packages tidyverse v.2.0.0, dplyr v.1.1.2, reshape2 v.1.4.4, and scales v.1.2.1. Principal component eigenvalues were calculated with the function prcomp. Sample distances for nonmetric dimensional scaling (NMDS) analysis were determined with the package vegan v.2.6-4; hierarchical clustering was done with functions dist() and hclust(). For statistical analysis, data were first assessed for normal distribution by performing visual inspection via density and *Q*–*Q* plots and normality testing with the Shapiro–Wilk method shapiro.test() in R. The type of data collected here was ratio data, and the groups were unpaired and normality testing indicated non-normal distribution of data in all cases. Hence, we performed Kruskal–Wallis tests via kruskal.test() and pairwise comparison via Mann–Whitney-Wilcoxon testing using the function pairwise.wilcox.test() to determine statistical differences between groups. Where appropriate, we used the multcompView package function multcompLetters() to assign multivariate comparisons into statistical groups denoted by letters. Heat maps were generated with the R package gplots v.3.1.3 using the function heatmap.2, dot plots, boxplots, and violin plots, which were done using the R package ggplot2 v.3.4.2 (Wickham, 2009). Venn diagrams were plotted with the online tool jvenn at https://jvenn.toulouse.inrae.fr/app/index.html (Bardou *et al.*, 2014).

Results

Selection of three partially *mlo*-virulent *B. hordei* isolates by experimental evolution

To study the rapid evolution of *B. hordei* experimentally, we selected for *mlo*-virulent *B. hordei* isolates derived from the *mlo*-avirulent parental strain *B. hordei* $K1_{AC}$. For 15 asexual generations, occasionally occurring *B. hordei* $K1_{AC}$ colonies on otherwise highly resistant barley *mlo* mutant plants were recovered, fungal biomass proliferated on the susceptible (*Mlo* genotype) cultivar (cv) Ingrid, and then conidia re-inoculated on *mlo* plants, as described before (Schwarzbach, 1979). Subsequently, from Generation 15 onwards, the resulting *B. hordei* isolates were cultivated on barley *mlo* mutant plants only, yielding the three independent strains Supervirulent K1 (SK1), SK2, and SK3. These isolates showed stable yet partial *mlo* virulence with visible sporulation and a 15–25% host cell entry rate on otherwise highly resistant barley *mlo*-3 backcrossed to cv Ingrid (BCI) mutant plants (Fig. 1a,b). *B. hordei* SK1 exhibited a similar level of virulence on a range of near-isogenic BCI *mlo* lines with various mutational defects in *Mlo* (Reinstädler *et al.*, 2010), indicating that in contrast to *B. hordei* RACE1 (Yaeno *et al.*, 2021), the enhanced virulence of this strain is independent of the host *mlo* allele (Figs 1c, S1). We found comparable host cell entry levels on two *mlo* mutants in different barley lines, Pallas *mlo*-5 (*c.* 15%) and Haisa *mlo*-1 (*c.* 20%; Fig. 1d), demonstrating that the *B. hordei* SK1 virulence phenotype is also independent of the

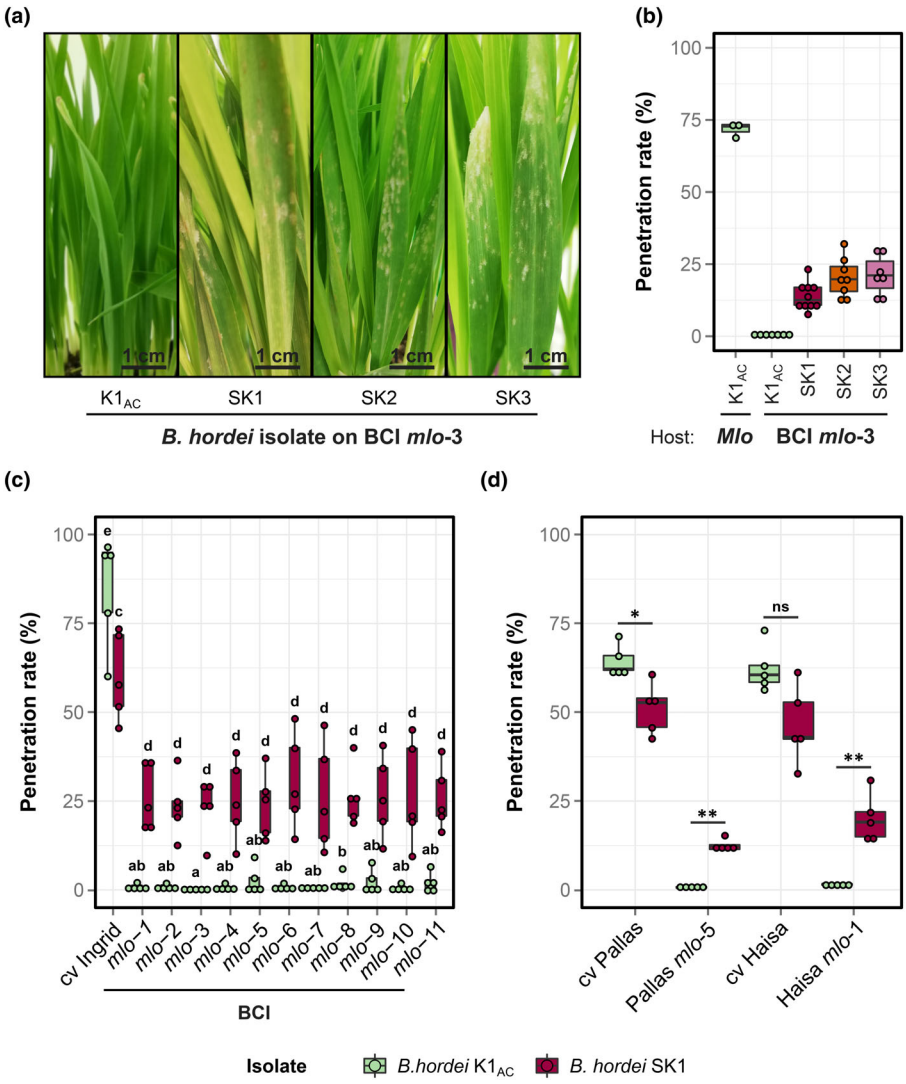

Fig. 1 Isolation of three partially *mlo*-virulent *Blumeria hordei* isolates. (a) Powdery mildew symptoms caused by *B. hordei* $K1_{AC}$ and *B. hordei* SK1, SK2, and SK3 at 7 d post inoculation (dpi) on barley backcross Ingrid (BCI) *mlo*-3 plants. (b) Penetration success in percent (%) of conidia from *B. hordei* $K1_{AC}$ (green) and the isolates *B. hordei* SK1 (maroon), SK2 (orange), and SK3 (purple) on the susceptible barley cv Ingrid (*Mlo*) or the BCI *mlo*-3 mutant lines. All data points are displayed. (c) Penetration success (%) of conidia from *B. hordei* $K1_{AC}$ (green) and SK1 (maroon) on the barley cultivar Ingrid and 11 different *mlo* mutant alleles backcrossed to Ingrid (BCI). (d) Penetration success (%) of conidia from *B. hordei* $K1_{AC}$ (green) and SK1 (blue) on barley *mlo*-5 and *mlo*-1 and the respective parental cultivars, cv Pallas and Haisa. Data are based on $n = 5$ independent replicates (c, d); at least 100 interactions per leaf, and three leaves were scored for each replicate. Center lines of box plots in b–d show the medians; upper and lower box limits indicate the 25th and 75th percentiles, respectively; upper and lower whiskers extend 1.5 times the interquartile range from the 25th and 75th percentiles, respectively, and dots represent the actual data (replicates). Letters denote statistical groups at $P < 0.05$ (c) according to Kruskal–Willis and Mann–Whitney–Wilcoxon testing. (d) *, $P < 0.05$; **, $P < 0.01$; ns, not significant.

host genetic background. We nevertheless noticed a slight (and in two cases statistically significant) reduction in *B. hordei* SK1 host cell entry rates compared with *B. hordei* $K1_{AC}$ on all WT (*Mlo*) genotypes tested (cv Ingrid, Pallas and Haisa; Fig. 1d), suggesting a lower pathogenic fitness of the *mlo*-virulent fungal isolate.

Enhanced virulence of *B. hordei* SK1 is restricted to *mlo* mutants in barley and *A. thaliana*

To assess whether *B. hordei* SK1 has a generally altered virulence spectrum, we inoculated various host (barley) and nonhost (*A. thaliana*) genotypes with conidia of this isolate and assessed the infection success. On barley BCI *mlo ror1* and *mlo ror2* double mutants, which have partially compromised *mlo* resistance due to second-site mutations in the genes *Ror1* and *Ror2* (Freialdenhoven *et al.*, 1996), the *mlo*-virulent isolate *B. hordei* SK1 showed elevated entry rates compared with *mlo* single mutant plants, indicative of an additive effect of the host *ror* mutations and the presumed genomic alterations in the fungal pathogen (Fig. S2). *B. hordei* SK1 showed reduced entry success not only on barley lines carrying *Mildew locus a* (*Mla*) alleles conferring isolate-specific immunity with different levels of effectiveness against *B. hordei* K1 (Jørgensen & Wolfe, 1994; Seeholzer *et al.*, 2010), but also on the near-isogenic control cultivars lacking the respective *Mla* genes (Fig. S3), suggesting that the isolate is incapable of overcoming race-specific resistance. *B. hordei* SK1 was further unable to colonize eight tested wheat cultivars and exhibited entry success levels comparable with *B. hordei* $K1_{AC}$, except on three cultivars where we observed a slight increase (Fig. S4A,B). Notably, *B. hordei* SK1 had significantly reduced penetration success on the *A. thaliana* mutants *pen2 pad4 sag101* and *pen1*, which are partially defective in resistance to the nonadapted *B. hordei* pathogen (Collins *et al.*, 2003; Lipka *et al.*, 2005), but increased entry success on the *A. thaliana mlo2* single mutant (Consonni *et al.*, 2006) and the *mlo2 mlo6 mlo12 pen1 pen2* quintuple mutant (Kuhn *et al.*, 2017). *B. hordei* SK1 even succeeded with occasional entry on the otherwise extremely resistant *mlo2 mlo6 mlo12* triple mutant (Consonni *et al.*, 2006), providing an additional link to *mlo* virulence also in the *B. hordei* nonhost species *A. thaliana* (Fig. S4C).

Blumeria hordei SK1 has an altered transcriptional profile during haustorium formation

To identify genes contributing to *mlo* virulence in *B. hordei* SK1 compared with *B. hordei* $K1_{AC}$, we performed whole transcriptome shotgun sequencing (RNA-seq) at 6 hpi (around appressorium formation) and 18 hpi (around haustorium establishment in compatible interactions; Table S2) using RNA extracted from inoculated barley (BCI *mlo*-3 genotype) leaf epidermal strips. The expression profiles of the host, representing the majority of the RNA-seq reads (> 90%), did not vary significantly between the barley epidermal samples inoculated with the two *B. hordei* isolates according to principal component analysis (PCA) and hierarchical distance calculations (hierarchical clustering and NMDS; Figs 2a, S5). However, PCA revealed a clear separation of the host responses at 6 hpi and 18 hpi, that is by time, but not by fungal isolate (K1 vs SK1; Fig. 2a). There were no differentially expressed (DE) host genes (inoculated by SK1 vs $K1_{AC}$) at 6 hpi and only nine DE host genes at 18 hpi (logFC > |1|, $P_{adj} < 0.05$; Fig. S6; Tables S3–S5). The low number of DE host genes might be explained by a still low proportion of successful fungal host cell entry events (*c.* 15–25%; Fig. 1a,b) and a high number of epidermal host cells not being attacked at all.

Between 282 167 (3.5%) and 1 472 273 (9.9%), RNA-seq read pairs mapped to the manually annotated *B. hordei* reference genome DH14 v.4 (Frantzeskakis *et al.*, 2018; Qian *et al.*, 2023) (Table S2). The expression profiles of *B. hordei* $K1_{AC}$ and SK1 were indistinguishable at 6 hpi but separated by fungal isolate at 18 hpi (Fig. 2b). Accordingly, while we did not identify DE *B. hordei* genes at 6 hpi, 127 genes were significantly ($P_{adj} < 0.05$; logFC > |1|) upregulated and two genes downregulated in *B. hordei* SK1 at 18 hpi compared with *B. hordei* $K1_{AC}$ (Figs 2c, S6; Tables S6, S7). Among the 127 upregulated genes, 95 (74.8%) code for proteins that harbor a canonical secretion signal (mostly putative effectors; Table S8). The two downregulated genes were *BLGH_02703* and *BLGH_06013*.

Next, we compared the expression profiles of the 129 DE genes in SK1 throughout the asexual life cycle in *B. hordei* on WT barley (cv Margret) plants. We took advantage of a publicly available RNA-seq dataset of *B. hordei* $K1_{AC}$ generated at six time points of the fungal infection cycle, ranging from spore germination to sporulation, that is 0, 6, 18, 24, 72, and 120 hpi (Qian *et al.*, 2023). Of the 127 genes formally upregulated in SK1 when grown on the *mlo*-3 mutant, 116 are usually expressed at 18 hpi in $K1_{AC}$ on a compatible host (Figs 2d, S7A; examples are shown in Figs 2e, S7B), suggesting failure of the *mlo*-avirulent isolate $K1_{AC}$ to induce these before or co-incident with haustorium establishment on barley *mlo* mutant plants. Of the remaining 11 genes formally upregulated in SK1, six were likewise induced by $K1_{AC}$ on the compatible host, but at later time points ('SK1 early'; Fig. 2d), while another five were specifically expressed in *B. hordei* SK1 but not in $K1_{AC}$ during the fungal infection cycle ('SK1-specific'; Figs 2d, S7B). These genes encoded putative secreted effector proteins (*BLGH_00850*, *BLGH_00851*, *BLGH_04339*, and *BLGH_07099*) and a gene of unknown function (*BLGH_05405*; Fig. S7B; Table S8). We validated the expression profiles of eight DE genes, including four which were specifically transcribed in *B. hordei* SK1 ('SK1-specific'; Fig. 2d) and the two downregulated genes (*BLGH_02703* and *BLGH_06013*; 'K1-specific'; Fig. 2d), by quantitative reverse transcription polymerase chain reaction. We found that most of these genes behaved like in SK1 in the *B. hordei* strains SK2 and SK3, pointing to a common transcriptomic signature during pathogenesis in the three *mlo*-virulent isolates (Figs 2f, S8). Based on the shared profile of DE genes, we hypothesize that the five genes specifically expressed in *B. hordei* SK1, SK2, and SK3 may play a pivotal role in enabling *mlo* virulence in *B. hordei*.

Three genes are co-affected by genomic events in the *mlo*-virulent *B. hordei* isolates

Next, we explored whether genomic alterations occur between the three *B. hordei* SK isolates and their parental (meta-) population (*B. hordei* $K1_{AC}$) using whole-genome shotgun sequencing (Table S9). We queried these genomes after at least 50 asexual generations when the *mlo* virulence phenotype had stabilized, since we expected purifying selection will have favored adaptive mutations to dominate within the fungal populations at this time. Compared with the near-chromosome level reference genome sequence of *B. hordei* DH14 (Frantzeskakis *et al.*, 2018), $K1_{AC}$ and SK1, SK2, and SK3 shared 140 639 single nucleotide variants (SNVs), 2137 of which were predicted to vary between the isolates. We manually confirmed 84 unambiguous polymorphisms, of which 81 were intergenic and three affected genes (Fig. 3a; Tables 1, S10). SK2 and SK3 only differed in one intergenic SNV, implying that the two isolates are genetically near-identical. The other variations include an SNV in *BLGH_06723* (encoding a putative conserved RBR-family E3 ubiquitin ligase), causing the change of glutamine-49 to lysine in all three *mlo*-virulent isolates, and a three-base pair (bp) deletion in the gene *BLGH_06013* in part of the SK1 population, causing the in-frame loss of lysine-445 (*BLGH_06013*$^{\Delta K445}$; Fig. 3b). *BLGH_06013* encodes the orthologue of *Aspergillus fumigatus* Af293 medA (medusa; BLASTP query cover 75%, identity 43.7%, *E* value 3E-112; GenBank accession XP_755658.1; Fig. S9). The abovementioned lysine-445 (lost in BLGH_06013 in part of the SK1 population) appears to represent a positionally conserved amino acid in nearly all fungal medA orthologues analyzed (Figs S10, S11).

We then calculated the average read coverage of all genes from the reference annotation (Frantzeskakis *et al.*, 2018), revealing two gene losses and two instances of copy number variation in the SK isolates (Fig. S12). One loss affected *BLGH_06013* and was due to deletion of an almost 40-kb region compared with *B. hordei* $K1_{AC}$ at scaffold_34 (422 240–451 834). While this region was completely absent in *B. hordei* SK2 and SK3, SK1 exhibited *c.* 50% loss of coverage, indicating a deletion present in part of the population (Fig. 3c). We reassembled scaffold_34 of SK1 using nanopore MinION sequencing (Table S11), which confirmed the deletion in a subset of the population with this long-read

sequencing technology and revealed the apparent *de novo* insertion of a *Tad1-9* retrotransposon at this site, replacing the 40-kb region (Fig. 3d). The second gene loss concerned *BLGH_02703* and was due to an 8-kb deletion in scaffold_23:1 727 078–1 735 005, where the reads again exhibited reduced (*c.* 50%) coverage in SK1 and complete absence of the locus in SK2 and SK3 (Fig. 3e). BLGH_02703 has no similarity to known proteins in the NCBI database except in the closely related wheat powdery mildew pathogen, *B. graminis* f.sp. *tritici* (EPQ63962; BLASTP query cover 92%, *E* value 2e-154, 68.3% sequence identity) and f.sp. *triticale* (CAD6506008; query cover 85%, *E* value 2e-166, 68.7% sequence identity), and otherwise has weak similarity to MSCRAMM family adhesin clumping factor ClfA, atrophin-1, K^+-dependent Na^+/Ca^{2+} exchanger, and a guanine nucleotide exchange factor (GEF) for Rho/Rac/Cdc42-like GTPases (Table S12). Both regions showing deletions in the SK isolates (in scaffolds 23 and 34) were flanked by long terminal repeat (LTR)-type transposable elements such as *Tad1*, *Ty3*, *Ty1/Copia*, and non-LTR4 (Fig. 3c,e). The partial absence of *BLGH_02703* (*Blumeria*-specific) and *BLGH_06013* (*medA*) within the *B. hordei* SK1 population likely accounts for the reduced transcript accumulation of these two genes seen in RNA-seq analysis at 18 hpi (Fig. 2d), since expression of both genes typically peaks at this time point in $K1_{AC}$ on a compatible barley host plant (Fig. 2f). We did not find the *BLGH_02703*, *BLGH_06013*, and *BLGH_6723* polymorphisms in the naturally *mlo*-virulent RACE1 isolate (Fig. S13), suggesting that its virulence is mechanistically different from *B. hordei* SK1 and SK2/3.

The copy number variations we detected in the SK isolates relative to the *B. hordei* DH14 reference genome (Frantzeskakis *et al.*, 2018) were limited to two loci (Figs S12, S14). Scaffold_27:312 420–348 900 encompasses *BLGH_05230*, *BLGH_05231*, and *BLGH_05232*, coding for a karyopherin nuclear transport factor, an aminopeptidase, and a glutathione peroxidase, respectively. The region exhibited *c.* twofold coverage by sequence reads of isolates $K1_{AC}$ and SK1 compared with the B. *hordei* DH14 reference genome and isolates SK2 and SK3. Likewise, sequence coverage indicated that the neighboring gene *BLGH_05233*, encoding a Sgk2-like serine–threonine kinase (Kusch *et al.*, 2014) and assembled as one copy in DH14, was represented by two copies in isolates *B. hordei* SK2 and SK3 instead of three copies in isolates *B. hordei* $K1_{AC}$ and SK1. Scaffold_8:1 787 835–1 794 235, containing *BLGH_00850*, whose encoded protein is 36.5% similar to the protein encoded by the adjacent gene *BLGH_00851* (CSEP0327, an effector candidate) and thus possibly a diverged copy thereof, was recently (probably in 2018) lost in our locally propagated *B. hordei* K1 population (*B. hordei* $K1_{AC}$) but not in the original *B. hordei* K1 population (*B. hordei* $K1_{CGN}$) and also not in the SK descendants derived from *B. hordei* $K1_{AC}$ (Figs S14B, S15). We confirmed the presence–absence polymorphisms of *BLGH_02703* (*Blumeria*-specific) and *BLGH_06013* (*medA*) by genotyping PCR and the $C^{222}A$ nucleotide exchange in *BLGH_06723* (E3 ubiquitin ligase) by Sanger sequencing of the PCR products (Figs 3f, S16). We summarized all genomic alterations detected in the three *B. hordei* SK isolates in Table 1.

Genomic variations emerge rapidly in the context of selection for *mlo* virulence in *B. hordei*

We conducted whole-genome resequencing of *B. hordei* isolates SK2 and SK3 at distinct stages of the selection process, that is at 5, 10, and 50 asexual generations under selection pressure on barley *mlo* mutant plants (Table S9). Most genomic variants described above were fixed in the *mlo*-virulent *B. hordei* populations, and the respective parental alleles were not detected any

Fig. 2 A distinct transcriptomic pattern is associated with *mlo* virulence of *Blumeria hordei* isolate SK1. We conducted RNA-seq of epidermal samples collected from barley backcross Ingrid (BCI) *mlo*-3 inoculated with *B. hordei* $K1_{AC}$ and SK1, respectively, at 6 h post inoculation (hpi) and 18 hpi, each with $n = 4$ independent replicates. (a) Hierarchical clustering dendrogram (upper panel) and principal component (PC) analysis (PCA; lower panel) of gene expression in barley *mlo*-3 in the 18 samples accounting for the four conditions. Green, K1; maroon, SK1; squares, 6 hpi; circles, 18 hpi. Numbers in brackets indicate the ratio of data explained by the principal component. (b) Hierarchical clustering dendrogram and PCA of gene expression in *B. hordei* $K1_{AC}$ and *B. hordei* SK1 at 6 hpi and 18 hpi on barley *mlo*-3. (c) Differential expression analysis revealed 127 upregulated and 2 downregulated genes in *B. hordei* SK1 at 18 hpi on barley BCI *mlo*-3 (Supporting Information Figs S6, S7; Table S7). The heat map shows the normalized relative expression (expressed as Row Z score, i.e. the distance between a data point and the mean) of these 129 genes in the two isolates at 6 and 18 hpi according to the color-coded scale at the bottom. Genes of particular interest within the heat map are indicated. (d) The illustration summarizes how the 129 differentially expressed (DE) SK1 genes compare with time-course gene expression data obtained for $K1_{AC}$ on the susceptible barley cv Margret (Qian *et al.*, 2023). Gray indicates genes that are induced in SK1 at 18 hpi on cv Margret but not expressed in $K1_{AC}$ on barley *mlo*-3; light blue indicates genes downregulated in $K1_{AC}$ at 18 hpi compared to 6 hpi; dark blue labels genes highly upregulated in SK1 at 18 hpi and upregulated at later time points (24 hpi or after) in $K1_{AC}$ on cv Margret; green indicates genes downregulated in SK1, which are upregulated in $K1_{AC}$ on cv Margret at 18 hpi; red highlights genes specifically expressed in SK1. The asterisk indicates genes that were induced in $K1_{AC}$ on cv Margret, but only at marginal levels < 50 transcripts per million (TPM; Fig. S7). (e) Dot plots show the expression of *BLGH_02703*, *BLGH_06013*, *BLGH_00851*, and *BLGH_06054* in TPM (*y*-axis) in *B. hordei* $K1_{AC}$ on the susceptible cv Margret in a time-course at 0, 6, 18, 24, 72, and 120 hpi (Qian *et al.*, 2023). (f) Data of quantitative reverse transcription polymerase chain reaction analysis for *BLGH_02703*, *BLGH_06013*, *BLGH_00851*, and *BLGH_06054* (upregulated in both isolates; see Fig. S7B for additional genes) for the isolates *B. hordei* $K1_{AC}$ (green), SK1 (maroon), SK2 (orange), and SK3 (purple) after inoculation of barley *mlo*-3. The *x*-axis shows the time point after inoculation (0, 6, and 18 hpi), the *y*-axis displays relative transcript abundance calculated by ΔC_t analysis. Data shown are based on $n = 3$ biological replicates with three technical replicates each. Center lines of box plots show the medians; upper and lower box limits indicate the 25th and 75th percentiles, respectively; upper and lower whiskers extend 1.5 times the interquartile range from the 25th and 75th percentiles, respectively, and dots represent the actual data (replicates).

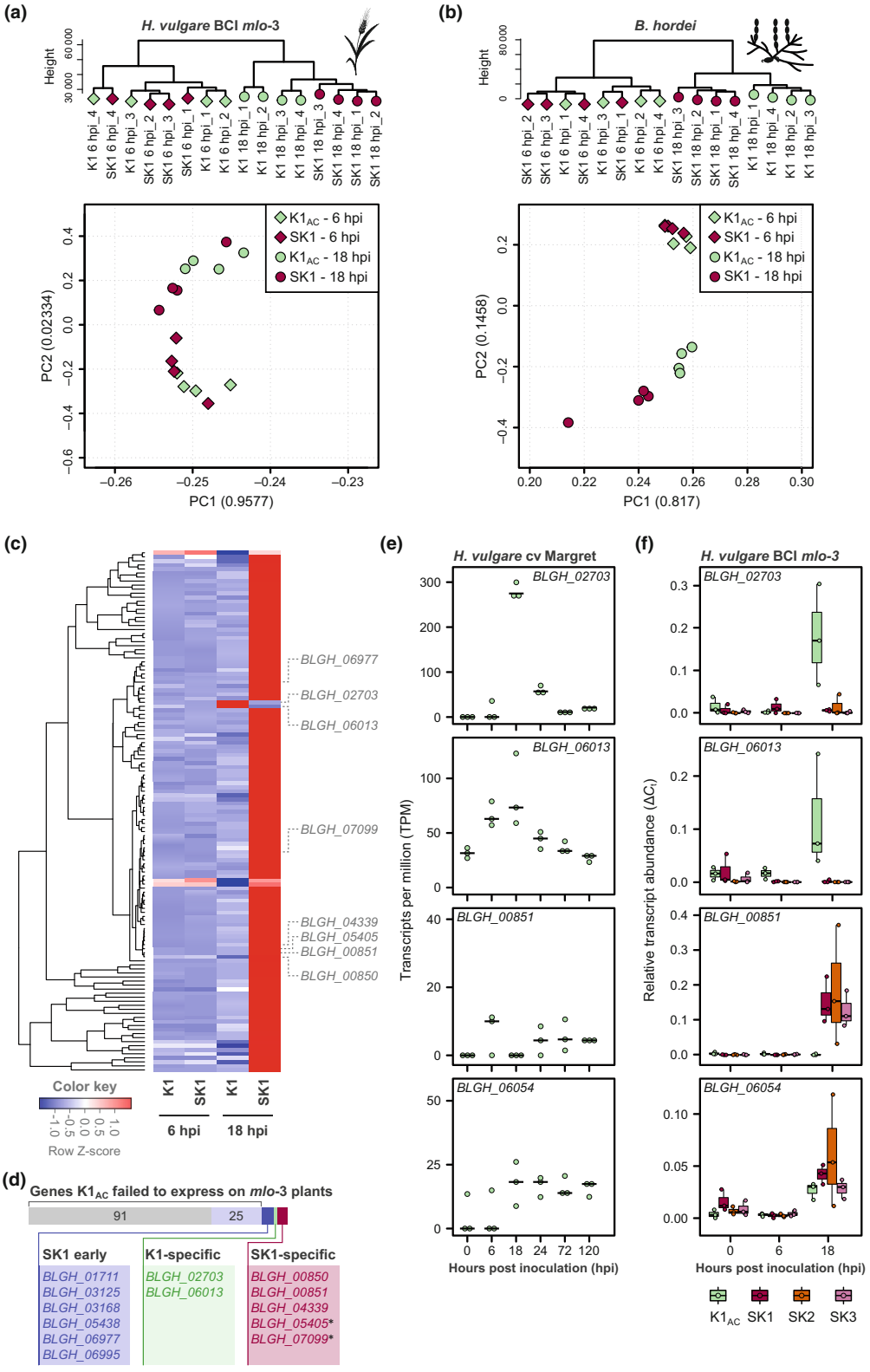

longer at Generation 50. To track the emergence and trajectory of the novel mutant alleles, we analyzed their frequency at asexual Generations 5 and 10 (Fig. S17). Of the 84 confirmed genomic variations (Table S10), 30 were already detectable at low frequencies in SK2 and 32 in SK3 at Generation 5, and their frequencies within the populations gradually increased to full penetrance by Generation 50. By contrast, 30 variations unique to $K1_{AC}$ but absent in SK1, SK2, and SK3 were also present at high frequencies at Generations 5 and 10, albeit with gradually decreasing frequencies. Likewise, the haplotype of the locus

containing *BLGH_00850* (Fig. S14B) was already detectable at low coverage in SK2 at Generation 10 and SK3 at Generation 5, and its frequency increased to full penetrance by Generation 50 (Fig. S18A). Another seven SNVs uniquely detected in $K1_{AC}$ were either absent or only detectable at frequencies < 1% at Generations 5 and 10 in SK2 and SK3, indicating their counterselection in these *mlo*-virulent isolates. By contrast, resequencing of $K1_{AC}$ after 5 yr (in 2023, equivalent to *c.* 250 asexual generations) confirmed that the 37 variations uniquely found in $K1_{AC}$ remained fixed in the *B. hordei* $K1_{AC}$ meta-population (Fig. S17A). Overall, the parallel gradual emergence or disappearance of alternative alleles in SK2 and SK3 suggest a

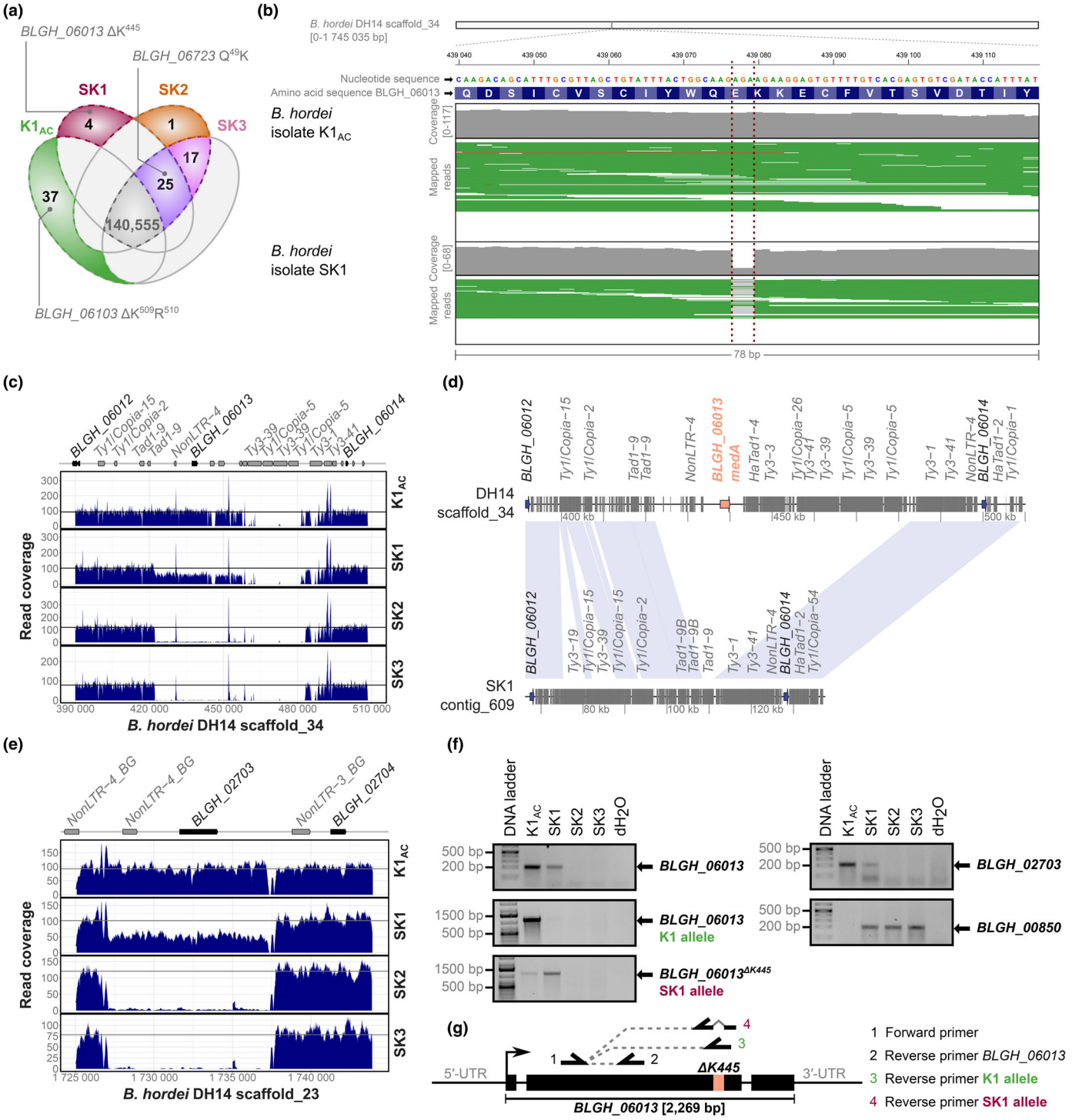

Fig. 3 Loss of genes *BLGH_06013* and *BLGH_02703* in *mlo*-virulent *Blumeria hordei* isolates. We performed high-throughput whole-genome DNA sequencing with the isolates *B. hordei* $K1_{AC}$, SK1, SK2, and SK3. (a) Venn diagram summarizing single nucleotide variants (SNVs) occurring in *B. hordei* K1, SK1, SK2, and SK3 relative to the reference genome of *B. hordei* DH14 v.4. All variants were confirmed by manual inspection, except the SNVs common in all four isolates (gray). SNVs affecting coding sequences are indicated. (b) SNVs were detected with Freebayes using an optimized pipeline for *Blumeria* (Barsoum *et al*., 2020) and visualized using the IGV browser (Robinson *et al*., 2017). The red lines highlight a variation (3-bp deletion) in *B. hordei* SK1 compared to $K1_{AC}$. White bar, scaffold_34 of the *B. hordei* DH14 reference assembly; below, the nucleotide and amino acid sequence of BLGH_06013 are shown. Mapping coverage is shown in gray, individual mapped reads are displayed in green, gaps in light gray. (c) Mapping coverage of *B. hordei* DH14 scaffold_34:390 000–510 000 of *B. hordei* $K1_{AC}$, SK1, SK2, and SK3, including the locus of *BLGH_06013*. The x-axis shows the position on the scaffold, the *y*-axis read coverage, and transposable elements are indicated at the top. The black line shows the average coverage for the respective isolate, site-specific coverage is displayed in dark blue. (d) Local synteny plot of scaffold_34:390 000–510 000 (*BLGH_06013* locus in orange). Genes are indicated by blue arrows and transposable elements by gray blocks. *B. hordei* DH14 scaffold_34 was assembled in *B. hordei* SK1 (sk1_contig_609) using nanopore MinION sequencing. (e) Mapping coverage of *B. hordei* DH14 scaffold_23:1 725 000–1 750 000 of *B. hordei* $K1_{AC}$, SK1, SK2, and SK3, including the locus of *BLGH_02703*. Displayed as in (c). (f) Genotyping PCRs for *BLGH_02703* and *BLGH_06013* alleles using genomic DNA of *B. hordei* $K1_{AC}$, SK1, SK2, and SK3, respectively. The gene *BLGH_00850* served as a positive control for PCR amplification. DNA Ladder, 1 kb plus (Invitrogen-Thermo Fisher, Waltham, MA, USA). (g) Primer locations for genotyping of *BLGH_06013*. Oligonucleotides are listed in Supporting Information Table S1.

Table 1 Mutational events detected in *B. hordei* SK1, SK2, and SK3.

Gene	*BLGH_06013*	*BLGH_06723*	*BLGH_02703*	*BLGH_05230 BLGH_05231 BLGH_05232*	*BLGH_05233*
Encoded protein	medA-like transcriptional regulator	E3 ubiquitin ligase	Unknown protein, *Blumeria*-specific	Nuclear transport factor (karyopherin)/ aminopeptidase/glutathione peroxidase	Sgk2-like serine–threonine protein kinase
B. hordei isolate					
$K1_{AC}$	n.v.[a]	n.v.	n.v.	2× coverage[b]	3× coverage[b]
SK1	Absent (partially) ΔK^{445} (partially)	$Q^{49}K$	Absent (partially)	2× coverage[b]	3× coverage[b]
SK2	Absent	$Q^{49}K$	Absent	1× coverage[b]	2× coverage[b]
SK3	Absent	$Q^{49}K$	Absent	1× coverage[b]	2× coverage[b]

[a]n.v., no variation compared with the *Blumeria hordei* reference isolate DH14 v.4.
[b]Relative to the *Blumeria hordei* reference isolate DH14 v.4.

subpopulation that pre-existed at low frequency in $K1_{AC}$ and that was positively selected and gave rise to the *mlo*-virulent strains.

Interestingly, neither of the variations observed for *BLGH_06013* (*medA*) could be observed at asexual Generations 5 and 10 in SK2/SK3 (Fig. S17B). The 3-bp deletion present in SK1 could not be found, and the read coverage of *BLGH_06013* was high at both time points. Similarly, read coverage for the gene *BLGH_02703* (*Blumeria*-specific) was high as well at Generations 5 and 10 (Fig. S18B), suggesting that the losses of *BLGH_06013* and *BLGH_02703* occurred after Generation 10 but were nonetheless fixed in the populations by Generation 50. In summary, the analysis of the SK isolates at various stages of the selection process supports the rapid initial emergence of genomic variants and a gradual shift in their allele frequencies toward the trait of stable *mlo* virulence.

Loss of *BLGH_02703* is dispensable for *mlo* virulence of *B. hordei* SK1

We next aimed to address whether the *mlo* virulence phenotype depends on the loss of genes *BLGH_02703* (*Blumeria*-specific) and/or *BLGH_06013* (*medA*), which are partially absent or mutated in the *B. hordei* SK1 population and both absent in SK2 and SK3 (Fig. 3; Table 1). Given the lack of reliable genetic tools for obligate biotrophic plant pathogens including powdery mildews, we took advantage of the nonhomogenous SK1 population to isolate single spore-derived and PCR-validated *B. hordei* genotypes. We succeeded in separating individual colonies that either carry or lack *BLGH_02703* (*Blumeria*-specific) in combination with either the *BLGH_06013* (*medA*) deletion or the $BLGH\_06013^{\Delta K445}$ variant (three different genotype combinations; Fig. 4a). The host cell entry success of these genotypes on *mlo* mutant leaves ranged from 5% to 12%, and there was no statistically significant difference in this respect between these isolates (Fig. 4b). By contrast, reminiscent of the original SK1 isolate (Fig. 1d), SK2, and SK3 as well as all SK1-derived genotypes showed reduced entry success on barley WT (*Mlo* genotype) leaves (Fig. 4c). Transient silencing of *BLGH_02703*, *BLGH_06013*, and *BLGH_06723*, separately or in combination, by particle bombardment-mediated host-induced gene silencing (Nowara *et al*., 2010) did not confer virulence to *B. hordei* K1 on barley *mlo*-3 leaves (Fig. S19). Taken together, these data indicate that the loss of *BLGH_02703* (*Blumeria*-specific) is not required for *B. hordei* to acquire *mlo* virulence.

Loss of *BLGH_06013* (*medA*) does not affect conidia morphology in *B. hordei*

The transcription factor medA is required for the formation of normal conidia in the ascomycete *Aspergillus fumigatus*, as *A. fumigatus medA* mutants display aberrations in conidia number and shape (Gravelat *et al*., 2010; Al Abdallah *et al*., 2012).

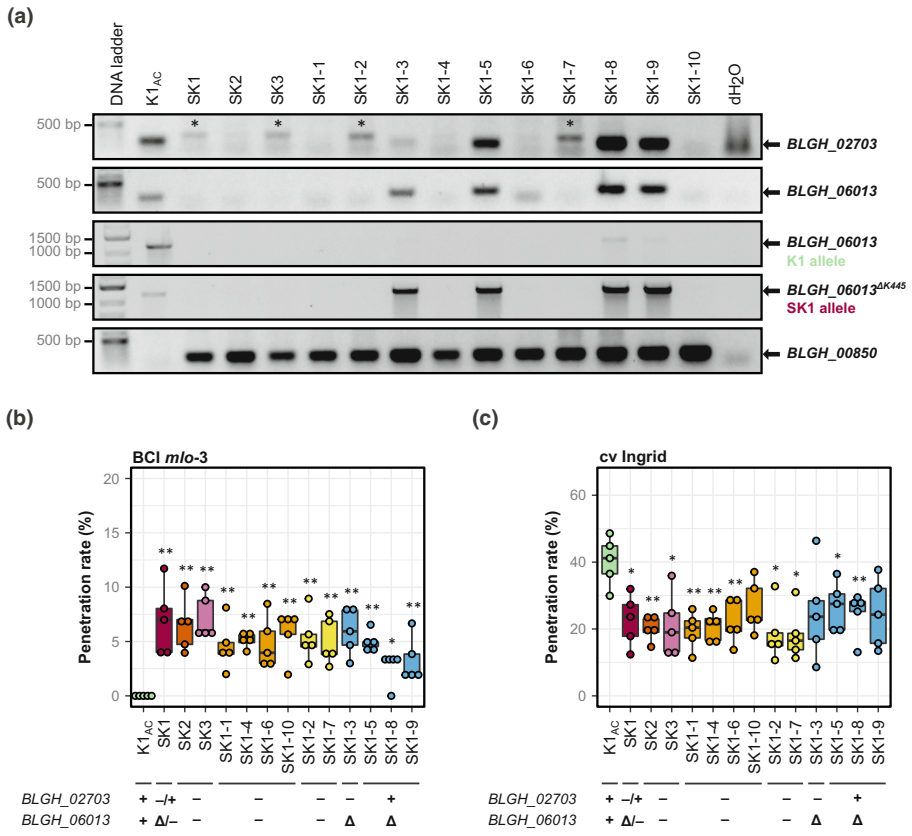

Fig. 4 Loss of *BLGH_02703* is dispensable for *mlo* virulence in *Blumeria hordei* SK1. Using the *B. hordei* SK1 meta-population, we captured several defined mutant genotypes and combinations thereof as single spore isolates. (a) Genotyping PCR for *BLGH_02703* and *BLGH_06013* with three different primer pairs as indicated in Fig. 3(g) on genomic DNA isolated from various *B. hordei* isolates. Asterisks indicate a sporadically occurring nonspecific PCR product in case of the *BLGH_02703* PCR; since the origin of these bands is unclear, lines with these bands are indicated in yellow in the boxplots in panels (b) and (c). Gene *BLGH_00850* served as a positive control for PCR amplification. (b, c) penetration success (%) of conidia from *B. hordei* isolates $K1_{AC}$ (green), SK1 (maroon), SK2 (orange), SK3 (purple), and the 10 isolates (light orange, yellow, and blue) analyzed in (a) on barley BCI *mlo*-3 (b) and cv Ingrid (*Mlo*) (c). Genotypes are color-coded as indicated below the panels (Δ indicates *BLGH_06013*$^{\Delta K445}$). Data are based on $n = 5$ independent replicates. At least 100 interactions per leaf and three leaves were scored for each replicate. Center lines of box plots show the medians; upper and lower box limits indicate the 25th and 75th percentiles, respectively; upper and lower whiskers extend 1.5 times the interquartile range from the 25th and 75th percentiles, respectively, and dots represent the actual data (replicates). Asterisks indicate statistically significant differences to $K1_{AC}$ at *, $P < 0.05$ and **, $P < 0.01$, according to Kruskal–Willis and Mann–Whitney–Wilcoxon statistical tests.

We therefore wondered whether the mutation(s) in *BLGH_06013* (*medA*) would likewise affect the morphology of asexual spores in the *B. hordei* SK isolates. While we observed uniform oval-shaped conidiospores in the case of *B. hordei* $K1_{AC}$, the *mlo*-virulent isolates SK1, SK2, and SK3 showed the presence of markedly elongated ellipse-shaped conidiospores (Fig. 5a). We, therefore, assessed essential conidia size parameters (length, width, and area) of the SK isolates in comparison with *B. hordei* $K1_{AC}$. All tested *mlo*-virulent genotypes (SK1, SK2, SK3, and the mutant combinations described above) had significantly increased conidia length (median 32–36 µm) compared with the parental isolate *B. hordei* $K1_{AC}$ (median 23 µm; Fig. S20). The same applied, in tendency, to conidia area (*c.* 213 µm^2 vs 160 µm^2), while conidia width of the SK isolates was indistinguishable from *B. hordei* $K1_{AC}$ conidia (both *c.* 11 µm; Fig. S20). However, when we assessed conidia shape of the *B. hordei* isolates $K1_{CGN}$, A6, DH14, and RACE1, we noticed that all these isolates had conidia longer than 30 µm on average, similar to SK1, SK2, and SK3 (Fig. 5b). Like *B. hordei* $K1_{AC}$, all of these isolates carried the WT allele of *BLGH_06013*, suggesting that the *B. hordei medA* ortholog is not responsible for the aberrant shape of conidia in *B. hordei* $K1_{AC}$, and that conidia morphology is not correlated with *mlo* virulence in isolates SK1, SK2, and SK3. The discrepancy in spore morphology between *B. hordei* $K1_{AC}$ and all other tested *B. hordei* isolates points toward a spontaneous mutation in $K1_{AC}$, affecting this trait that must have occurred and became fixed in the population after the isolation of the SK isolates.

mlo virulence may cause an overall fitness penalty in *B. hordei*

We had noticed early on that the virulent isolate *B. hordei* SK1 displayed a reduced entry rate compared with $K1_{AC}$ on barley cultivars carrying a functional *Mlo* gene (Fig. 1d). To test the viability of conidia, we allowed the conidia of *B. hordei* K1, SK1,

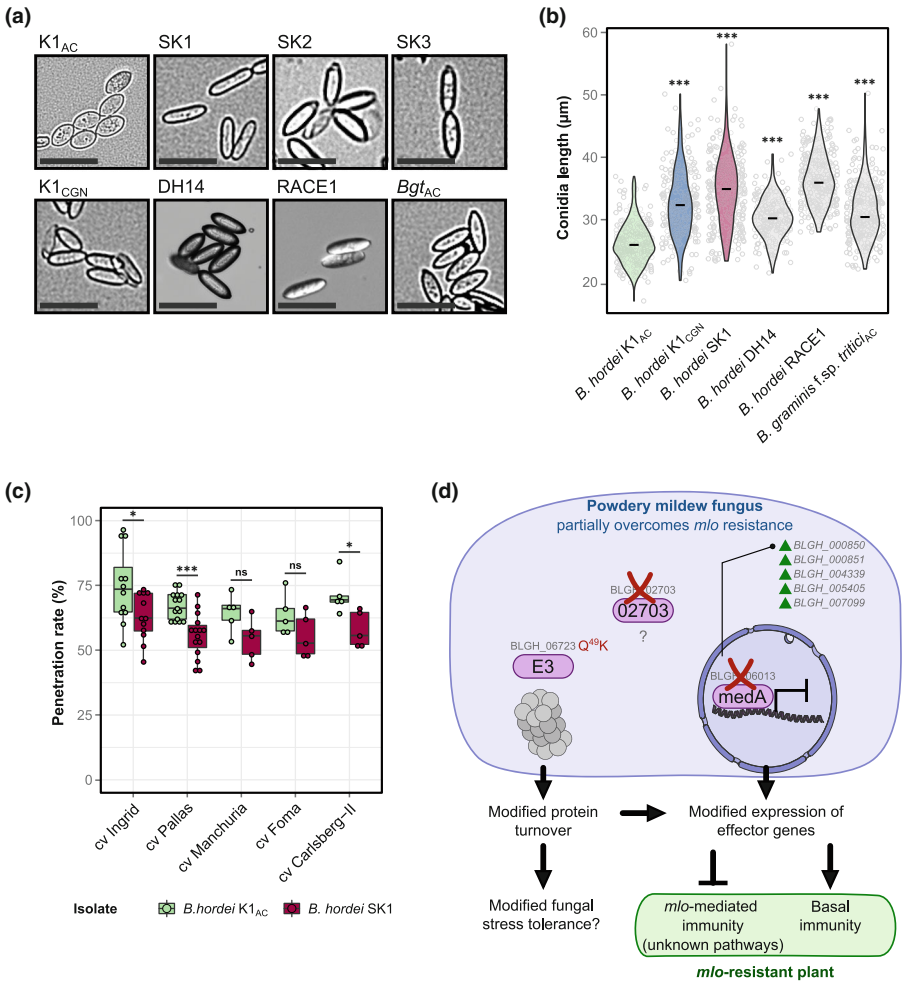

Fig. 5 The loss of *BLGH_06013* does not affect conidiospore morphology. (a) Representative micrographs of conidia (brightfield); Bars, 50 µm. Conidia were obtained from *Blumeria hordei* $K1_{AC}$, SK1, SK2, SK3, $K1_{CGN}$, DH14 (courtesy by Pietro Spanu, Imperial College London), RACE1, and *B. graminis* f.sp. *tritici*. (b) The violin plot shows the length of conidia (µm) (*y*-axis) for *B. hordei* $K1_{AC}$, SK1, $K1_{CGN}$, DH14, RACE1, and *B. graminis* f.sp. *tritici* isolate Aachen (*Bg tritici*$_{AC}$). The center lines of the violin plots show the median; the curved lines indicate the shape of the distribution; the dots represent the data points (measured conidia). At least 300 conidia were measured for each isolate. A statistical test according to Mann–Whitney-Wilcoxon was performed to estimate differences to $K1_{AC}$; ***, $P < 0.001$. (c) Penetration success (%) of conidia from *B. hordei* $K1_{AC}$ (green) and SK1 (maroon) on barley cultivars (*Mlo* genotype) Ingrid ($n = 12$), Pallas ($n = 15$), Manchuria, Foma, and Carlsberg-II ($n = 5$ independent replicates each). Center lines of box plots show the medians; upper and lower box limits indicate the 25th and 75th percentiles, respectively; upper and lower whiskers extend 1.5 times the interquartile range from the 25th and 75th percentiles, respectively, and dots represent the actual data (replicates). Statistical analysis was performed comparing SK1 with K1 on the respective cultivar using Kruskal–Willis and Mann–Whitney–Wilcoxon statistical tests; *, $P < 0.05$; ***, $P < 0.001$; ns, not significant. (d) Simplified model for partial *mlo* virulence in the barley powdery mildew pathogen. Multiple pathways contribute to *mlo*-based resistance against powdery mildew pathogens. Our experiments demonstrated that *mlo* virulence in *B. hordei* SK1 is additive to suppression of resistance by loss of known defense pathways, suggesting a different mechanism that leads to successful infection. We identified three genomic variations in the partially *mlo*-virulent *B. hordei* isolates SK1 and SK2/3. These encode the proteins E3 ubiquitin ligase BLGH_06723, which may be involved in protein turnover, the transcriptional regulator BLGH_06013 (medA), whose absence or non-functionality may allow the activation of several genes including candidate effector-encoding genes, and a third *Blumeria*-specific protein of unknown function (BLGH_02703). Note that loss of BLGH_02703 does not seem to be required for partial *mlo* virulence (Fig. 4). We postulate that the E3 ligase BLGH_06723 and the transcriptional regulator medA alter the infection program of *B. hordei* SK1 and SK2/3 to collectively enable colonization of *mlo*-resistant barley. We observed that *B. hordei* SK1 remained avirulent on barley *Mla* lines effective against K1 (Supporting Information Fig. S3) as well as on nonhost wheat cultivars (Fig. S4), indicating that *mlo*-mediated resistance and *mlo* virulence are mechanistically distinct from effector-triggered and basal immunity. Since the *mlo*-virulent isolates are less virulent on susceptible barley *Mlo* plants, we suggest that suppression of *mlo*-mediated immunity might be accompanied by less effective suppression of basal plant immunity. Purple ovals symbolize the three proteins found to be lacking/mutated in the three *B. hordei* SK1 isolates. Blunt arrows indicate suppression, standard arrows contribution to the indicated process; the red 'X' signifies absence of a functional allele encoding for the respective protein. The schematic was generated using icons from https://bioicons.com: proteasome icon by jaiganesh (https://github.com/jaiganeshjg); nucleus-full-3d and dna-5 icon icons by Servier (https://smart.servier.com/).

SK2, SK3, and the various genotypes isolated from the SK1 meta-population to germinate on agar medium. Under these *in vitro* conditions, *c.* 50–75% of conidia formed germ tubes. The majority of the SK isolates displayed normal or slightly enhanced germination rates (*c.* 50–70%; Fig. S20B), indicating that germination and formation of the primary germ tube

remained largely unaffected between *mlo*-virulent isolates and by the aberrant conidia shape in $K1_{AC}$. Then, we analyzed a set of barley cultivars susceptible to *B. hordei* K1 and carrying a functional *Mlo* allele to compare the entry success of the two isolates *B. hordei* $K1_{AC}$ and SK1. Intriguingly and consistent with our other experimental data (Figs 1d, 4c), *B. hordei* SK1 showed a significantly reduced entry success with a decrease of *c.* 5–15% compared with *B. hordei* $K1_{AC}$ on these cultivars, suggesting a fitness penalty for *B. hordei* SK1 (Fig. 5c). To assess whether *B. hordei* $K1_{AC}$ would rapidly outcompete *B. hordei* SK1 as a consequence of this fitness penalty, we performed competition experiments. However, *B. hordei* $K1_{AC}$ did not outcompete *B. hordei* SK1 in these settings, and *mlo*-virulent *B. hordei* isolates did not lose their *mlo* virulence after 12 generations of propagation on WT barley leaves (cv Ingrid; *Mlo* genotype), that is in the absence of the selective pressure (Fig. S21).

Discussion

Experimental evolution can be a powerful tool to study genome evolution in plant-associated fungal microbes (Manriquez *et al.*, 2021). Using this approach, we discovered a single amino acid exchange in one gene and the loss of two genes co-occurring in all three *B. hordei* SK isolates (Table 1). This mutational spectrum correlates with the gain of virulence on otherwise highly powdery mildew-resistant barley *mlo* mutant plants, which confer a type of broad-spectrum resistance that mechanistically differs from isolate-specific immunity conferred by NLR proteins (Peterhänsel *et al.*, 1997; Humphry *et al.*, 2006). Different from mutations leading to the loss of NLR-mediated isolate-specific resistance, none of these genes code for effectors but rather a RBR-family E3 ubiquitin ligase (BLGH_06723), a medA-like transcriptional regulator (BLGH_06013), and a *Blumeria*-specific protein of unknown function (BLGH_02703). The $Q^{49}K$ substitution in BLGH_06723 does not affect a conserved amino acid and is not located in an annotated functional domain of the protein (Fig. S22). We can, however, not exclude that this missense mutation leads to either a nonfunctional version or a gain-of-function variant, or, alternatively, affects the stability and accumulation levels of the protein. Our analyses based on the segregating SK1 population demonstrated that the lack of *BLGH_02703* is dispensable for both *mlo* virulence and the conidiospore morphology phenotype (Figs 4, 5). Likewise, the copy number variation of genes *BLGH_05230*, *BLGH_05231*, *BLGH_05232*, and *BLGH_05233* is restricted to *B. hordei* SK2 and SK3 and not found in SK1 (Table 1). These genomic variations are thus unlikely to be causative for *mlo* virulence. This leaves the $Q^{49}K$ substitution in BLGH_06723 (E3 ubiquitin ligase) and/or the mutation/absence of BLGH_06013 (medA) as the most probable alterations conferring partial *mlo* virulence in the *B. hordei* SK isolates. The lack of genetic tools for the obligate biotrophic powdery mildew pathogens at present prevents a more rigorous testing of the candidate genes, for example by targeted gene knockouts or complementation analysis.

It is intriguing that all three *B. hordei* SK isolates share an almost identical set of adaptive mutations, including the joint occurrence of a single amino acid substitution in *BLGH_06723* (Table 1). Similarly, previously isolated *B. hordei* isolates depended on three unidentified genes that unequally contributed to *mlo* virulence (Atzema, 1998; Grell *et al.*, 2005). These earlier experiments resulted in strains of three distinctive levels of virulence, suggesting at least three major adaptive mutations (Schwarzbach, 1979). This observation prompts the question whether the SK isolates represent independent mutational events, and whether the detected sequence variants might pre-exist as balanced polymorphisms within the *B. hordei* $K1_{AC}$ population or whether they are independently and convergently acquired *de novo* events that were selected for during experimental evolution. Since isolate SK1 on the one hand and SK2/SK3 on the other hand were retrieved more than 2 yr apart from each other and differ in the mutational spectrum detected for *BLGH_06013* (*medA*) and the copy number variation of *BLGH_05230*, *BLGH_05231*, *BLGH_05232*, and *BLGH_05233* (Table 1), we can assume at least two independent and convergent sets of adaptive mutational events. By contrast, isolates SK2 and SK3 are near-identical and according to our analysis only differ by one validated SNV in an intergenic region, suggesting that these two isolates might have the same origin. It may thus well be possible that a founder event for *mlo* virulence (e.g. the $Q^{49}K$ substitution in BLGH_06723) is present at low levels as a balanced polymorphism within the parental *B. hordei* $K1_{AC}$ population, which may give rise to sporadic colony formation on *mlo* plants. One or more additional events, such as the loss-of-function *BLGH_06013* (*medA*), might be required to stabilize virulence on *mlo* mutant plants. While we found no evidence for the BLGH_06723 $Q^{49}K$ variant to be present in the K1 population, we detected > 70 SNVs including this one at asexual Generation 5 after start of the experimental selection at low frequencies in both SK2 and SK3, while variants in *BLGH_06013* and *BLGH_02703* were not detectable, supporting the hypothesis of a founder population in which *mlo* virulence is later stabilized by additional events. This notion is further strengthened by the earlier experimental evolution approaches conducted by Erik Schwarzbach, who likewise observed discrete stepwise increases in *mlo* virulence in the course of the experiment (Schwarzbach, 1979). Developing targeted PCR methods to detect the mutational events such as the BLGH_06723 $Q^{49}K$ variant, in both laboratory and field populations, could help to further substantiate the hypothesis of pre-existing founder populations and have implications for future disease control in barley.

Gene loss is often associated with adaptation to new host environments and host jumps in fungal pathogens (Sharma *et al.*, 2014). Various processes could facilitate the rapid gain and loss of genes in *B. hordei*. Genome recombination due to mating (sexual reproduction) can promote genetic diversity, which, for example, gave rise to the emergence of *B. graminis* f.sp. *triticale* by hybridization of wheat and rye powdery mildews (Menardo *et al.*, 2016). However, we isolated the *mlo*-virulent strains from asexually reproducing populations. Thus, the extensive repertoire of transposable elements (Frantzeskakis *et al.*, 2018) is the most likely driver of rapid genomic changes in the fungus. We noted that in the case of *BLGH_06013* a *Tad1-9* transposon appears to

have replaced the locus containing this gene in SK1 (Fig. 3d), suggesting that transposition of a *Tad1* element caused genome rearrangement at this site, consistent with the copy–paste mechanism of retroelements (Wicker *et al.*, 2007). However, the transposition itself would not explain the loss of a large genomic segment. While nonhomologous end joining (NHEJ) is the dominant mechanism to repair double-strand breaks in genomic DNA in haploid genomes (Rodgers & McVey, 2016; Chang *et al.*, 2017), it accounts predominantly for insertions and deletions (indels) of < 20 bp. Microhomologies, however, can cause long-distance template switching due to replication fork collapse during cell division, which can frequently occur in repetitive and AT-rich regions (Vissers *et al.*, 2009; Bose *et al.*, 2014). The resulting DNA end intermediates can be stabilized and repaired by microhomology-mediated end joining (MMEJ), which in this case uses microhomologies from nonhomologous templates and is therefore error-prone (Stankiewicz & Lupski, 2002; Hastings *et al.*, 2009; Carvalho & Lupski, 2016). Microhomology-driven replication-based DNA repair mechanisms such as microhomology-mediated end joining cause large-scale insertions, deletions, and copy number variation (Payen *et al.*, 2008; Sakofsky *et al.*, 2015; Ebert & Fields, 2020). Since powdery mildew genomes are enriched with repetitive elements including retrotransposons that exhibit little sequence divergence (Wicker *et al.*, 2013; Frantzeskakis *et al.*, 2018), microhomologies likely occur frequently and could give rise to extensive structural variation in the fungus. Typically, virulence genes encoding effectors, carbohydrate-processing enzymes (CAZymes), and toxins are often found in the vicinity of transposable elements, frequently embedded within transposon-rich genome compartments (Dong *et al.*, 2015; Frantzeskakis *et al.*, 2019; Badet & Croll, 2020). For example, population-wide screening of the gene content in the Septoria leaf blotch pathogen *Zymoseptoria tritici* identified 599 gene gains and 1024 gene losses, which mainly occurred in subtelomeric regions and in proximity to transposable elements. The majority of these genes encode virulence factors, secreted proteins, and enzymes involved in the biosynthesis of secondary metabolites (Hartmann & Croll, 2017). Inaccurate microhomology-based repair of double-strand breaks occurring in the transposon-rich and repetitive regions may be one major driver of copy number variation of genes coding for effectors and other virulence factors.

Why do the mutational events observed in the *B. hordei* SK isolates not occur naturally in barley powdery mildew populations in the field? This might be explained by the fact that the affected isolates show reduced infection success on susceptible (*Mlo* WT) barley genotypes (Fig. 5d). Due to the adverse effects of this adaptation, such strains may not emerge in a nonselective environment where susceptible barley genotypes are available as hosts. It is conceivable that the rotation of *mlo*-resistant and nonresistant spring and winter varieties, respectively, as currently practiced by farmers in European agriculture (Jørgensen, 1992), results in the absence of constant selection pressure, thereby preventing the occurrence of natural *mlo*-virulent strains so far. Given the rapidity with which *mlo* virulence appeared under our laboratory conditions, we caution against the permanent deployment of barley *mlo* mutants without rotation to prevent the appearance of *mlo*-virulent barley powdery mildew in agricultural settings.

In summary, we established experimental evolution as a novel addition to the genetic toolbox available to study obligate biotrophic pathogens such as powdery mildew fungi. This approach complements the recently established mutagenesis pipelines (Barsoum *et al.*, 2020; Bernasconi *et al.*, 2024). The complex (meta-) population structures of fungal isolates (Barsoum *et al.*, 2020), which confounds genomic analyses, and the lack of effective transformation systems for the validation of candidate genes nonetheless remain challenges for the work with these organisms.

Acknowledgements

Seeds of the wheat cultivars used in this study were kindly provided by the late Patrick Schweizer (IPK Gatersleben, Germany) and Beat Keller (Zürich University, Switzerland). We thank Bernd Denecke (IZKF Aachen) for permitting access to the Illumina NextSeq sequencer and the Agilent Bioanalyzer platform. We acknowledge Alexander Vogel, Bianca Reiß, and Björn Usadel (RWTH Aachen University) for access to DNA quantification via Qubit. The analysis was performed with computing resources granted by RWTH Aachen University under project ID rwth0146. This study was supported by the RWTH Aachen Excellence Initiative (RWTH Fellow grant to RP) and funded by the Deutsche Forschungsgemeinschaft (DFG, German Research Foundation) project no. 274444799 (grants 861/14-1 and 861/14-2 awarded to RP) in the context of the DFG-funded priority program SPP1819 'Rapid evolutionary adaptation – potential and constraints'. Open Access funding enabled and organized by Projekt DEAL.

Competing interests

None declared.

Author contributions

RP and SK designed the study; RP, LF and SK were responsible for experiment conception. LP isolated *B. hordei* SK1, LF and MB *B. hordei* SK2 and SK3. SK, BDL and KDW performed the pathogen assays. LF generated the samples for RNA-seq, SK analyzed the quantitative data and the RNA-seq data. SK, LF and MB prepared high-molecular-weight genomic DNA of the *B. hordei* strains. LF, MB and SK performed genome assemblies, comparative genomics, and subsequent data analysis. FK sampled and isolated RNA for quantitative reverse transcription polymerase chain reaction, performed quantitative reverse transcription polymerase chain reaction, and cloned the *BLGH_06013* alleles. SK wrote the first draft of the manuscript and SK and RP edited the manuscript; LF provided critical feedback on the drafts. All authors read the manuscript and approved the final version.

ORCID

Mirna Barsoum https://orcid.org/0000-0003-0838-8137

Lamprinos Frantzeskakis https://orcid.org/0000-0001-8947-6934
Florian Kümmel https://orcid.org/0009-0006-2169-0890
Stefan Kusch https://orcid.org/0000-0002-2472-5255
Ralph Panstruga https://orcid.org/0000-0002-3756-8957
Lina Pesch https://orcid.org/0000-0002-1828-7447

Data availability

All raw RNA and DNA sequencing data generated in this study are deposited at https://www.ebi.ac.uk/ena under project ID PRJEB36770 (*B. hordei* $K1_{AC}$ (Barsoum *et al.*, 2020)) and at https://www.ncbi.nlm.nih.gov/sra under BioProject ID PRJNA639160. The draft genome assembly for *B. hordei* SK1 has been deposited at DDBJ/ENA/GenBank under the accession no. JAJOCF000000000.

References

Acevedo-Garcia J, Spencer D, Thieron H, Reinstädler A, Hammond-Kosack KE, Phillips AL, Panstruga R. 2017. *mlo*-based powdery mildew resistance in hexaploid bread wheat generated by a non-transgenic TILLING approach. *Plant Biotechnology Journal* **15**: 367–378.

Acevedo-Garcia J, Walden K, Leissing F, Baumgarten K, Drwiega K, Kwaaitaal M, Reinstädler A, Freh M, Dong X, James GV *et al.* 2022. Barley *Ror1* encodes a class XI myosin required for *mlo*-based broad-spectrum resistance to the fungal powdery mildew pathogen. *The Plant Journal* **112**: 84–103.

Al Abdallah Q, Choe S-I, Campoli P, Baptista S, Gravelat FN, Lee MJ, Sheppard DC. 2012. A conserved C-terminal domain of the *Aspergillus fumigatus* developmental regulator MedA is required for nuclear localization, adhesion and virulence. *PLoS ONE* **7**: e49959.

Atzema JL. 1998. *Durability of* mlo *resistance in barley against powdery mildew caused by* Erysiphe graminis *f.sp.* hordei. PhD thesis, ETH Zürich. doi: 10.3929/ethz-a-002054806.

Badet T, Croll D. 2020. The rise and fall of genes: Origins and functions of plant pathogen pangenomes. *Current Opinion in Plant Biology* **56**: 65–73.

Bardou P, Mariette J, Escudié F, Djemiel C, Klopp C. 2014. JVENN: an interactive Venn diagram viewer. *BMC Bioinformatics* **15**: 293.

Barsoum M, Kusch S, Frantzeskakis L, Schaffrath U, Panstruga R. 2020. Ultraviolet mutagenesis coupled with next-generation sequencing as a method for functional interrogation of powdery mildew genomes. *Molecular Plant–Microbe Interactions* **33**: 1008–1021.

Bernasconi Z, Stirnemann U, Heuberger M, Sotiropoulos AG, Graf J, Wicker T, Keller B, Sánchez-Martín J. 2024. Mutagenesis of wheat powdery mildew reveals a single gene controlling both NLR and tandem kinase-mediated immunity. *Molecular Plant–Microbe Interactions* **37**: 264–276.

Bolger AM, Lohse M, Usadel B. 2014. TRIMMOMATIC: a flexible trimmer for Illumina sequence data. *Bioinformatics* **30**: 2114–2120.

Bose P, Hermetz KE, Conneely KN, Rudd MK. 2014. Tandem repeats and G-rich sequences are enriched at human CNV breakpoints. *PLoS ONE* **9**: e101607.

Braun U, Cook RTA. 2012. *Taxonomic manual of the Erysiphales (Powdery Mildews)*. Utrecht, the Netherlands: CBS-KNAW Fungal Biodiversity Centre.

Brown JKM. 2015. Durable resistance of crops to disease: a Darwinian perspective. *Annual Review of Phytopathology* **53**: 513–539.

Büschges R, Hollricher K, Panstruga R, Simons G, Wolter M, Frijters A, van Daelen R, Van Der Lee TAJ, Diergaarde P, Groenendijk J *et al.* 1997. The barley *Mlo* gene: a novel control element of plant pathogen resistance. *Cell* **88**: 695–705.

Carvalho CMB, Lupski JR. 2016. Mechanisms underlying structural variant formation in genomic disorders. *Nature Reviews Genetics* **17**: 224–238.

Chang HHY, Pannunzio NR, Adachi N, Lieber MR. 2017. Non-homologous DNA end joining and alternative pathways to double-strand break repair. *Nature Reviews Molecular Cell Biology* **18**: 495–506.

Cingolani P, Platts A, Wang LL, Coon M, Nguyen T, Wang L, Land SJ, Lu X, Ruden DM. 2012. A program for annotating and predicting the effects of single nucleotide polymorphisms, SnpEff: SNPs in the genome of *Drosophila melanogaster* strain w1118; *iso*-2; *iso*-3. *Fly* **6**: 80–92.

Collins NC, Thordal-Christensen H, Lipka V, Bau S, Kombrink E, Qiu J-L, Hückelhoven R, Stein M, Freialdenhoven A, Somerville SC *et al.* 2003. SNARE-protein-mediated disease resistance at the plant cell wall. *Nature* **425**: 973–977.

Consonni C, Humphry ME, Hartmann HA, Livaja M, Durner J, Westphal L, Vogel J, Lipka V, Kemmerling B, Schulze-Lefert P *et al.* 2006. Conserved requirement for a plant host cell protein in powdery mildew pathogenesis. *Nature Genetics* **38**: 716–720.

Danecek P, Auton A, Abecasis G, Albers CA, Banks E, DePristo MA, Handsaker RE, Lunter G, Marth GT, Sherry ST *et al.* 2011. The variant call format and VCFtools. *Bioinformatics* **27**: 2156–2158.

Dean RA, Van Kan JAL, Pretorius ZA, Hammond-Kosack KE, Di Pietro A, Spanu PD, Rudd JJ, Dickman M, Kahmann R, Ellis J *et al.* 2012. The top 10 fungal pathogens in molecular plant pathology. *Molecular Plant Pathology* **13**: 414–430.

Devoto A, Hartmann HA, Piffanelli P, Elliott C, Simmons C, Taramino G, Goh C-S, Cohen FE, Emerson BC, Schulze-Lefert P *et al.* 2003. Molecular phylogeny and evolution of the plant-specific seven-transmembrane MLO family. *Journal of Molecular Evolution* **56**: 77–88.

Dong S, Raffaele S, Kamoun S. 2015. The two-speed genomes of filamentous pathogens: Waltz with plants. *Current Opinion in Genetics and Development* **35**: 57–65.

Ebert D, Fields PD. 2020. Host–parasite co-evolution and its genomic signature. *Nature Reviews Genetics* **21**: 754–768.

Erdős G, Pajkos M, Dosztányi Z. 2021. IUPred3: prediction of protein disorder enhanced with unambiguous experimental annotation and visualization of evolutionary conservation. *Nucleic Acids Research* **49**: W297–W303.

Feehan JM, Scheibel KE, Bourras S, Underwood W, Keller B, Somerville SC. 2017. Purification of high molecular weight genomic DNA from powdery mildew for long-read sequencing. *Journal of Visualized Experiments* **121**: e55463.

Flor HH. 1971. Current status of the gene-for-gene concept. *Annual Review of Phytopathology* **9**: 275–296.

Frantzeskakis L, Di Pietro A, Rep M, Schirawski J, Wu C, Panstruga R. 2020. Rapid evolution in plant–microbe interactions – a molecular genomics perspective. *New Phytologist* **225**: 1134–1142.

Frantzeskakis L, Kracher B, Kusch S, Yoshikawa-Maekawa M, Bauer S, Pedersen C, Spanu PD, Maekawa T, Schulze-Lefert P, Panstruga R. 2018. Signatures of host specialization and a recent transposable element burst in the dynamic one-speed genome of the fungal barley powdery mildew pathogen. *BMC Genomics* **19**: 381.

Frantzeskakis L, Kusch S, Panstruga R. 2019. The need for speed: compartmentalized genome evolution in filamentous phytopathogens. *Molecular Plant Pathology* **20**: 3–7.

Freialdenhoven A, Peterhänsel C, Kurth J, Kreuzaler F, Schulze-Lefert P. 1996. Identification of genes required for the function of non-race-specific *mlo* resistance to powdery mildew in barley. *Plant Cell* **8**: 5–14.

Gao Q, Wang C, Xi Y, Shao Q, Li L, Luan S. 2022. A receptor–channel trio conducts Ca^{2+} signalling for pollen tube reception. *Nature* **607**: 534–539.

Garrison E, Marth G. 2012. Haplotype-based variant detection from short-read sequencing. *arXiv*. doi: 10.48550/arXiv.1207.3907.

Glawe DA. 2008. The powdery mildews: a review of the world's most familiar (yet poorly known) plant pathogens. *Annual Review of Phytopathology* **46**: 27–51.

Gravelat FN, Ejzykowicz DE, Chiang LY, Chabot JC, Urb M, Macdonald KD, Al-Bader N, Filler SG, Sheppard DC. 2010. *Aspergillus fumigatus* MedA governs adherence, host cell interactions and virulence. *Cellular Microbiology* **12**: 473–488.

Grell MN, Holm KB, Giese H. 2005. Two novel *Blumeria graminis* f. sp. *hordei* genes are induced *in planta* and up-regulated in *mlo* virulent isolates. *Physiological and Molecular Plant Pathology* **66**: 79–89.

Guy L, Roat Kultima J, Andersson SGE. 2010. genoPlotR: comparative gene and genome visualization in R. *Bioinformatics* **26**: 2334–2335.

Hacquard S, Kracher B, Maekawa T, Vernaldi S, Schulze-Lefert P, van Themaat EVL. 2013. Mosaic genome structure of the barley powdery mildew pathogen and conservation of transcriptional programs in divergent hosts. *Proceedings of the National Academy of Sciences, USA* **110**: E2219–E2228.

Hartmann FE, Croll D. 2017. Distinct trajectories of massive recent gene gains and losses in populations of a microbial eukaryotic pathogen. *Molecular Biology and Evolution* **34**: 2808–2822.

Hastings PJ, Ira G, Lupski JR. 2009. A microhomology-mediated break-induced replication model for the origin of human copy number variation. *PLoS Genetics* **5**: e1000327.

Hématy K, Lim M, Cherk C, Piślewska-Bednarek M, Sanchez-Rodriguez C, Stein M, Fuchs R, Klapprodt C, Lipka V, Molina A *et al.* 2020. Moonlighting function of Phytochelatin Synthase1 in extracellular defense against fungal pathogens. *Plant Physiology* **182**: 1920–1932.

Hinze K, Thompson RD, Ritter E, Salamini F, Schulze-Lefert P. 1991. Restriction fragment length polymorphism-mediated targeting of the *ml-o* resistance locus in barley (*Hordeum vulgare*). *Proceedings of the National Academy of Sciences, USA* **88**: 3691–3695.

Humphry ME, Consonni C, Panstruga R. 2006. *mlo*-based powdery mildew immunity: silver bullet or simply non-host resistance? *Molecular Plant Pathology* **7**: 605–610.

Jones JDG, Dangl JL. 2006. The plant immune system. *Nature* **444**: 323–329.

Jørgensen JH. 1992. Discovery, characterization and exploitation of *Mlo* powdery mildew resistance in barley. *Euphytica* **63**: 141–152.

Jørgensen JH, Wolfe M. 1994. Genetics of powdery mildew resistance in barley. *Critical Reviews in Plant Sciences* **13**: 97–119.

Kim D, Langmead B, Salzberg SL. 2015. HISAT: a fast spliced aligner with low memory requirements. *Nature Methods* **12**: 357–360.

Kim MC, Panstruga R, Elliott C, Müller J, Devoto A, Yoon HW, Park HC, Cho MJ, Schulze-Lefert P. 2002. Calmodulin interacts with MLO protein to regulate defence against mildew in barley. *Nature* **416**: 447–451.

Kuhn H, Lorek J, Kwaaitaal M, Consonni C, Becker K, Micali C, Ver Loren van Themaat E, Bednarek P, Raaymakers TM, Appiano M *et al.* 2017. Key components of different plant defense pathways are dispensable for powdery mildew resistance of the Arabidopsis *mlo2 mlo6 mlo12* triple mutant. *Frontiers in Plant Science* **8**: 1006.

Kumar S, Stecher G, Tamura K. 2016. MEGA7: molecular evolutionary genetics analysis v.7.0 for bigger datasets. *Molecular Biology and Evolution* **33**: 1870–1874.

Kurtz S, Phillippy A, Delcher AL, Smoot M, Shumway M, Antonescu CM, Salzberg SL. 2004. Versatile and open software for comparing large genomes. *Genome Biology* **5**: R12.

Kusch S, Ahmadinejad N, Panstruga R, Kuhn H. 2014. *In silico* analysis of the core signaling proteome from the barley powdery mildew pathogen (*Blumeria graminis* f.sp. *hordei*). *BMC Genomics* **15**: 843.

Kusch S, Panstruga R. 2017. *Mlo*-based resistance: An apparently universal 'weapon' to defeat powdery mildew disease. *Molecular Plant–Microbe Interactions* **30**: 179–189.

Kusch S, Qian J, Loos A, Kümmel F, Spanu PD, Panstruga R. 2024. Long-term and rapid evolution in powdery mildew fungi. *Molecular Ecology* **33**: e16909.

Langner T, Harant A, Gomez-Luciano LB, Shrestha RK, Malmgren A, Latorre SM, Burbano HA, Win J, Kamoun S. 2021. Genomic rearrangements generate hypervariable mini-chromosomes in host-specific isolates of the blast fungus. *PLoS Genetics* **17**: e1009386.

Law CW, Alhamdoosh M, Su S, Smyth GK, Ritchie ME. 2016. RNA-seq analysis is easy as 1-2-3 with limma, Glimma and edgeR. *F1000Research* **5**: 1408.

Li H, Durbin R. 2009. Fast and accurate short read alignment with Burrows–Wheeler transform. *Bioinformatics* **25**: 1754–1760.

Li H, Handsaker B, Wysoker A, Fennell T, Ruan J, Homer N, Marth G, Abecasis G, Durbin R. 2009. The sequence alignment/map format and SAMtools. *Bioinformatics* **25**: 2078–2079.

Li L, Collier B, Spanu P. 2019. Isolation of powdery mildew haustoria from infected barley. *Bio-Protocol* **9**: e3299.

Liao Y, Smyth GK, Shi W. 2014. featureCounts: an efficient general purpose program for assigning sequence reads to genomic features. *Bioinformatics* **30**: 923–930.

Lipka V, Dittgen J, Bednarek P, Bhat RA, Wiermer M, Stein M, Landtag J, Brandt W, Rosahl S, Scheel D *et al.* 2005. Pre- and postinvasion defenses both contribute to nonhost resistance in Arabidopsis. *Science* **310**: 1180–1183.

Liu M, Braun U, Takamatsu S, Hambleton S, Shoukouhi P, Bisson KR, Hubbard K. 2021. Taxonomic revision of *Blumeria* based on multi-gene DNA sequences, host preferences and morphology. *Mycoscience* **62**: 143–165.

Livak KJ, Schmittgen TD. 2001. Analysis of relative gene expression data using real-time quantitative PCR and the $2^{-\Delta\Delta CT}$ method. *Methods* **25**: 402–408.

Love MI, Huber W, Anders S. 2014. Moderated estimation of fold change and dispersion for RNA-seq data with DESeq2. *Genome Biology* **15**: 550.

Lu X, Kracher B, Saur IML, Bauer S, Ellwood SR, Wise RP, Yaeno T, Maekawa T, Schulze-Lefert P. 2016. Allelic barley MLA immune receptors recognize sequence-unrelated avirulence effectors of the powdery mildew pathogen. *Proceedings of the National Academy of Sciences, USA* **113**: E6486–E6495.

Lyngkjær MF, Jensen HP, Østergård H. 1995. A Japanese powdery mildew isolate with exceptionally large infection efficiency on *mlo*-resistant barley. *Plant Pathology* **44**: 786–790.

Manriquez B, Muller D, Prigent-Combaret C. 2021. Experimental evolution in plant-microbe systems: a tool for deciphering the functioning and evolution of plant-associated microbial communities. *Frontiers in Microbiology* **12**: 896.

Mascher M, Wicker T, Jenkins J, Plott C, Lux T, Koh CS, Ens J, Gundlach H, Boston LB, Tulpová Z *et al.* 2021. Long-read sequence assembly: a technical evaluation in barley. *Plant Cell* **33**: 1888–1906.

Menardo F, Praz CR, Wyder S, Ben-David R, Bourras S, Matsumae H, McNally KE, Parlange F, Riba A, Roffler S *et al.* 2016. Hybridization of powdery mildew strains gives rise to pathogens on novel agricultural crop species. *Nature Genetics* **48**: 201–205.

Müller MC, Kunz L, Graf JP, Schudel S, Keller B. 2021. Host adaptation through hybridization: Genome analysis of triticale powdery mildew reveals unique combination of lineage-specific effectors. *Molecular Plant–Microbe Interactions* **34**: 1350–1357.

Müller MC, Praz CR, Sotiropoulos AG, Menardo F, Kunz L, Schudel S, Oberhänsli S, Poretti M, Wehrli A, Bourras S *et al.* 2019. A chromosome-scale genome assembly reveals a highly dynamic effector repertoire of wheat powdery mildew. *New Phytologist* **221**: 2176–2189.

Newton AC, Young IM. 1996. Temporary partial breakdown of *Mlo*-resistance in spring barley by the sudden relief of soil water stress. *Plant Pathology* **45**: 973–977.

Nowara D, Gay A, Lacomme C, Shaw J, Ridout CJ, Douchkov D, Hensel G, Kumlehn J, Schweizer P. 2010. HIGS: host-induced gene silencing in the obligate biotrophic fungal pathogen *Blumeria graminis*. *Plant Cell* **22**: 3130–3141.

Payen C, Koszul R, Dujon B, Fischer G. 2008. Segmental duplications arise from Pol32-dependent repair of broken forks through two alternative replication-based mechanisms. *PLoS Genetics* **4**: e1000175.

Pennington HG, Li L, Spanu PD. 2015. Identification and selection of normalization controls for quantitative transcript analysis in *Blumeria graminis*. *Molecular Plant Pathology* **17**: 625–633.

Peterhänsel C, Freialdenhoven A, Kurth J, Kolsch R, Schulze-Lefert P. 1997. Interaction analyses of genes required for resistance responses to powdery mildew in barley reveal distinct pathways leading to leaf cell death. *Plant Cell* **9**: 1397–1409.

Qian J, Ibrahim HMM, Erz M, Kümmel F, Panstruga R, Kusch S. 2023. Long noncoding RNAs emerge from transposon-derived antisense sequences and may contribute to infection stage-specific transposon regulation in a fungal phytopathogen. *Mobile DNA* **14**: 17.

Quinlan AR, Hall IM. 2010. BEDTools: a flexible suite of utilities for comparing genomic features. *Bioinformatics* **26**: 841–842.

Qutob D, Tedman-Jones J, Dong S, Kuflu K, Pham H, Wang Y, Dou D, Kale SD, Arredondo FD, Tyler BM *et al.* 2009. Copy number variation and

transcriptional polymorphisms of *Phytophthora sojae* RXLR effector genes *Avr1a* and *Avr3a*. *PLoS ONE* **4**: e5066.

R Core Team. 2018. *R: a language and environment for statistical computing*. Vienna, Austria: R Foundation for Statistical Computing.

Raffaele S, Farrer RA, Cano LM, Studholme DJ, MacLean D, Thines M, Jiang RHY, Zody MC, Kunjeti SG, Donofrio NM *et al.* 2010. Genome evolution following host jumps in the Irish potato famine pathogen lineage. *Science* **330**: 1540–1543.

Reinstädler A, Müller J, Czembor JH, Piffanelli P, Panstruga R. 2010. Novel induced mlo mutant alleles in combination with site-directed mutagenesis reveal functionally important domains in the heptahelical barley Mlo protein. *BMC Plant Biology* **10**: 31.

Robinson JT, Thorvaldsdóttir H, Wenger AM, Zehir A, Mesirov JP. 2017. Variant review with the integrative genomics viewer. *Cancer Research* **77**: e31–e34.

Robinson MD, McCarthy DJ, Smyth GK. 2010. EDGER: a Bioconductor package for differential expression analysis of digital gene expression data. *Bioinformatics* **26**: 139–140.

Rodgers K, McVey M. 2016. Error-prone repair of DNA double-strand breaks. *Journal of Cellular Physiology* **231**: 15–24.

Sakofsky CJ, Ayyar S, Deem AK, Chung W-H, Ira G, Malkova A. 2015. Translesion polymerases drive microhomology-mediated break-induced replication leading to complex chromosomal rearrangements. *Molecular Cell* **60**: 860–872.

Saur IM, Bauer S, Kracher B, Lu X, Franzeskakis L, Müller MC, Sabelleck B, Kümmel F, Panstruga R, Maekawa T *et al.* 2019. Multiple pairs of allelic MLA immune receptor-powdery mildew AVRA effectors argue for a direct recognition mechanism. *eLife* **8**: e44471.

Schwarzbach E. 1979. Response to selection for virulence against the *ml-o* based mildew resistance in barley, not fitting the gene-for-gene hypothesis. *Barley Genetics Newsletter* **9**: 85–89.

Schwarzbach E. 2001. Heat induced susceptibility of *mlo*-barley to powdery mildew (*Blumeria graminis* D.C. f.sp. *hordei* Marchal). *Czech Journal of Genetics and Plant Breeding* **37**: 82–87.

Seeholzer S, Tsuchimatsu T, Jordan T, Bieri S, Pajonk S, Yang W, Jahoor A, Shimizu KK, Keller B, Schulze-Lefert P. 2010. Diversity at the *Mla* powdery mildew resistance locus from cultivated barley reveals sites of positive selection. *Molecular Plant–Microbe Interactions* **23**: 497–509.

Sharma R, Mishra B, Runge F, Thines M. 2014. Gene loss rather than gene gain is associated with a host jump from monocots to dicots in the smut fungus *Melanopsichium pennsylvanicum*. *Genome Biology and Evolution* **6**: 2034–2049.

Spanu PD, Abbott JC, Amselem J, Burgis TA, Soanes DM, Stüber K, van Themaat EVL, Brown JKM, Butcher SA, Gurr SJ *et al.* 2010. Genome expansion and gene loss in powdery mildew fungi reveal tradeoffs in extreme parasitism. *Science* **330**: 1543–1546.

Stankiewicz P, Lupski JR. 2002. Genome architecture, rearrangements and genomic disorders. *Trends in Genetics* **18**: 74–82.

Stein M, Dittgen J, Sánchez-Rodríguez C, Hou B-H, Molina A, Schulze-Lefert P, Lipka V, Somerville SC. 2006. Arabidopsis PEN3/PDR8, an ATP binding cassette transporter, contributes to nonhost resistance to inappropriate pathogens that enter by direct penetration. *Plant Cell* **18**: 731–746.

Tellier A, Moreno-Gámez S, Stephan W. 2014. Speed of adaptation and genomic footprints of host-parasite coevolution under arms race and trench warfare dynamics. *Evolution* **68**: 2211–2224.

Trempe J-F, Sauve V, Grenier K, Seirafi M, Tang MY, Ménade M, Al-Abdul-Wahid S, Krett J, Wong K, Kozlov G *et al.* 2013. Structure of parkin reveals mechanisms for ubiquitin ligase activation. *Science* **340**: 1451–1455.

Vissers LELM, Bhatt SS, Janssen IM, Xia Z, Lalani SR, Pfundt R, Derwinska K, de Vries BBA, Gilissen C, Hoischen A *et al.* 2009. Rare pathogenic microdeletions and tandem duplications are microhomology-mediated and stimulated by local genomic architecture. *Human Molecular Genetics* **18**: 3579–3593.

Waterhouse AM, Procter JB, Martin DMA, Clamp M, Barton GJ. 2009. JALVIEW v.2 – a multiple sequence alignment editor and analysis workbench. *Bioinformatics* **25**: 1189–1191.

Wiberg A. 1974. Genetical studies of spontaneous sources of resistance to powdery mildew in barley. *Hereditas* **77**: 89–148.

Wicker T, Oberhänsli S, Parlange F, Buchmann JP, Shatalina M, Roffler S, Ben-David R, Doležel J, Šimková H, Schulze-Lefert P *et al.* 2013. The wheat powdery mildew genome shows the unique evolution of an obligate biotroph. *Nature Genetics* **45**: 1092–1096.

Wicker T, Sabot F, Hua-Van A, Bennetzen JL, Capy P, Chalhoub B, Flavell A, Leroy P, Morgante M, Panaud O *et al.* 2007. A unified classification system for eukaryotic transposable elements. *Nature Reviews Genetics* **8**: 973–982.

Wickham H. 2009. In: Gentleman R, Hornik K, Parmigiani G, eds. *GGPLOT2: elegant graphics for data analysis*. New York, NY, USA: Springer-Verlag.

Yaeno T, Wahara M, Nagano M, Wanezaki H, Toda H, Inoue H, Eishima A, Nishiguchi M, Hisano H, Kobayashi K *et al.* 2021. RACE1, a Japanese *Blumeria graminis* f. sp. *hordei* isolate, is capable of overcoming partially *mlo*-mediated penetration resistance in barley in an allele-specific manner. *PLoS ONE* **16**: e0256574.

Supporting Information

Additional Supporting Information may be found online in the Supporting Information section at the end of the article.

Fig. S1 *Blumeria hordei* SK1 exhibits partial virulence on *mlo* mutant plants in different barley genetic backgrounds.

Fig. S2 *mlo* virulence of *Blumeria hordei* SK1 is independent of known prepenetration resistance pathways.

Fig. S3 *mlo* virulence of *Blumeria hordei* SK1 does not undermine race-specific resistance in barley.

Fig. S4 *mlo* virulence of *Blumeria hordei* SK1 does not enable colonization of the nonhost plants wheat and *Arabidopsis thaliana*.

Fig. S5 RNA-seq sample similarity analysis.

Fig. S6 *Blumeria hordei* SK1 exhibits differential expression on barley backcross Ingrid *mlo*-3 at 18 h post inoculation.

Fig. S7 One hundred and sixteen genes upregulated in *mlo*-virulent *Blumeria hordei* SK1 are usually expressed in *B. hordei* on a susceptible host.

Fig. S8 *mlo*-virulent isolates *Blumeria hordei* SK1, SK2, and SK3 display similar gene induction profiles.

Fig. S9 BLGH_06013 is the orthologue of *Aspergillus fumigatus* medA.

Fig. S10 K445 appears to be conserved in medA proteins.

Fig. S11 Sequences of BLGH_06013 (medA) proteins are near-identical between *Blumeria hordei* isolates.

Fig. S12 *mlo*-virulent strains of *Blumeria hordei* exhibit gene loss and copy number variation.

Fig. S13 Genetic basis for *mlo* virulence in *Blumeria hordei* SK1, SK2, and SK3 is distinct from *B. hordei* RACE1.

Fig. S14 Two loci exhibiting a deletion or copy number variation in *Blumeria hordei*.

Fig. S15 *BLGH_00850* was lost recently in the isolate *Blumeria hordei* $K1_{AC}$.

Fig. S16 *Blumeria hordei* SK1, SK2, and SK3 carry a $C^{222}A$ polymorphism in the coding sequence of *BLGH_06723*, causing a Q49K amino acid exchange of the encoded E3 ubiquitin ligase protein.

Fig. S17 Genomic variations appear rapidly upon adaptation to *mlo* resistance in *Blumeria hordei*.

Fig. S18 Genomic variations in *Blumeria hordei* strains.

Fig. S19 Host-induced gene silencing of *BLGH_06013*, *BLGH_06723*, and *BLGH_02703* does not confer *mlo* virulence in isolate *Blumeria hordei* K1.

Fig. S20 Loss of the transcriptional regulator *BLGH_06013* (*medA*) does not affect conidiospore formation.

Fig. S21 *mlo* virulence remains stable in *Blumeria hordei* in the absence of selection pressure.

Fig. S22 BLGH_06723 is a conserved RBR-type E3 ubiquitin ligase.

Table S1 List of oligonucleotides used in this study.

Table S2 RNA-seq mapping statistics.

Table S3 Differential expression analysis results of *Hordeum vulgare* backcross Ingrid *mlo*-3 at 6 h post inoculation with *Blumeria hordei* SK1 and $K1_{AC}$.

Table S4 Differential expression analysis results of *Hordeum vulgare* backcross Ingrid *mlo*-3 at 18 h post inoculation with *Blumeria hordei* SK1 and $K1_{AC}$.

Table S5 Annotations of differentially expressed genes in *Hordeum vulgare* backcross Ingrid *mlo*-3 at 18 h post inoculation.

Table S6 Differential expression analysis results of *Blumeria hordei* SK1 compared to *B. hordei* $K1_{AC}$ on *Hordeum vulgare* backcross Ingrid *mlo*-3 at 6 h post inoculation.

Table S7 Differential expression analysis results of *B. hordei* SK1 compared to *B. hordei* $K1_{AC}$ on *Hordeum vulgare* backcross Ingrid *mlo*-3 at 18 h post inoculation.

Table S8 Annotations of differentially expressed genes in *Blumeria hordei* SK1 at 18 h post inoculation.

Table S9 Whole-genome shotgun DNA sequencing mapping statistics.

Table S10 List of SNVs detected and manually inspected in $K1_{AC}$, SK1, SK2, and SK3 and their allele frequencies.

Table S11 Genome assembly statistics for *Blumeria hordei* SK1 compared with publicly available *B. hordei* genome assemblies.

Table S12 NCBI C-DART results for the protein BLGH_02703.

Please note: Wiley is not responsible for the content or functionality of any Supporting Information supplied by the authors. Any queries (other than missing material) should be directed to the *New Phytologist* Central Office.